*Graphical Abstract

IR Spectroscopy of cationized aliphatic amino acids: Stability of charge-solvated structure increases with metal cation size

Miriam K. Drayß[1], P. B. Armentrout[2], Jos Oomens[3,4] * and Mathias Schäfer[1] *

[1]Department of Chemistry, University of Cologne, Greinstraße 4, 50939 Köln, Germany;
[2]Department of Chemistry, University of Utah, 315 S. 1400 E. Rm 2020, Salt Lake City, Utah, USA
[3]FOM-Institute for Plasma Physics *Rijnhuizen,* Edisonbaan 14, NL-3439 MN Nieuwegein,
The Netherlands;
[4]University of Amsterdam, Nieuwe Achtergracht 166, 1018WV Amsterdam, The Netherlands

International Journal of Mass Spectrometry 2010

Stability trend of charge-solvated versus salt-bridge structures in alkali metal cationization is reversed for aliphatic versus functionalized amino acids as shown by IRMPD-spectroscopy and computational modeling

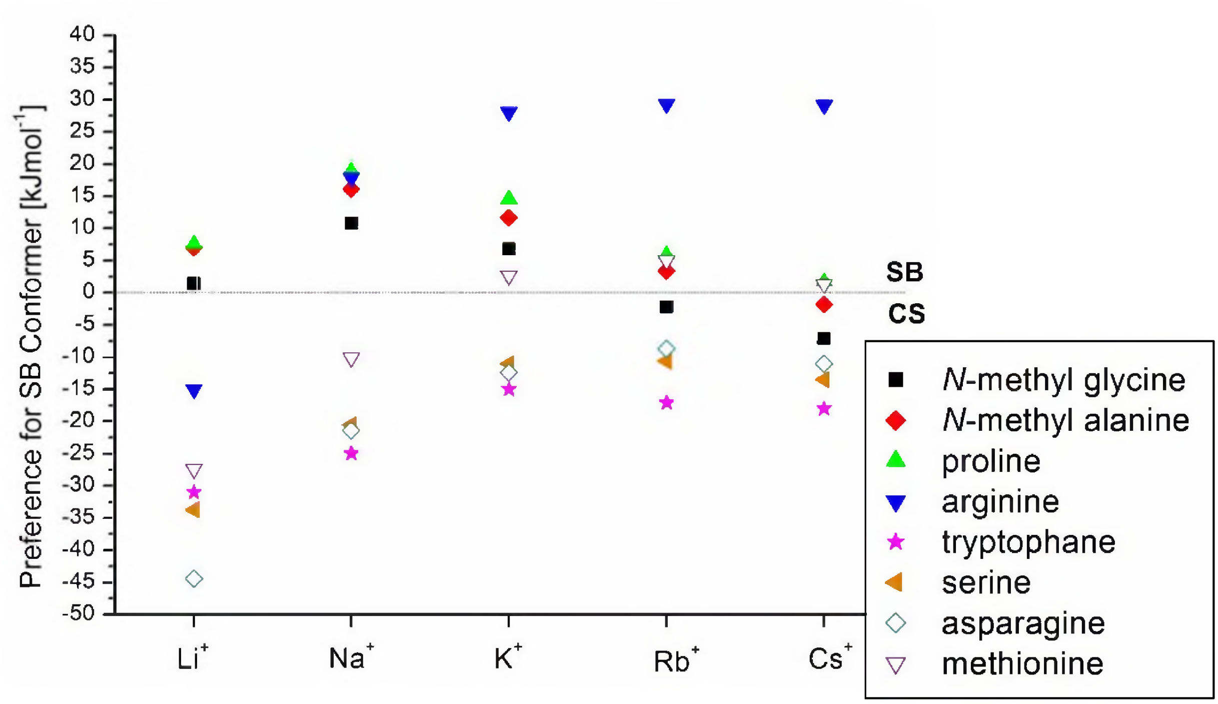

IR Spectroscopy of cationized aliphatic amino acids: Stability of charge-solvated structure increases with metal cation size

Miriam K. Drayß[1], P. B. Armentrout[2], Jos Oomens[3,4] * and Mathias Schäfer[1] *

[1]Department of Chemistry, University of Cologne, Greinstraße 4, 50939 Köln, Germany;
[2]Department of Chemistry, University of Utah, 315 S. 1400 E. Rm 2020, Salt Lake City, Utah, USA
[3]FOM-Institute for Plasma Physics *Rijnhuizen,* Edisonbaan 14, NL-3439 MN Nieuwegein, The Netherlands;
[4]University of Amsterdam, Nieuwe Achtergracht 166, 1018WV Amsterdam, The Netherlands

Corresponding authors

Jos Oomens
FOM-Institute for Plasma Physics *Rijnhuizen,* Edisonbaan 14, NL-3439 MN Nieuwegein,
The Netherlands, Fax: (+31)30-603 1204, e-mail: J.Oomens@rijnhuizen.nl

Mathias Schäfer
Department of Chemistry, University Cologne, Greinstraße 4, 50939 Köln, Germany, Fax: (+49)221-470 3064, e-mail: mathias.schaefer@uni-koeln.de

Abstract

Gas-phase structures of alkali metal cationized (Li^+, Na^+, K^+, Rb^+, Cs^+) proline (Pro) and *N*-methyl alanine have been investigated using infrared multiple photon dissociation (IRMPD) spectroscopy utilizing light generated by a free electron laser and computational modeling. Measured IRMPD spectra are compared to spectra calculated at the B3LYP/6-311++G(2d,2p) level of theory to identify individual conformers. Calculations indicate that the stability of the salt bridge (SB; *zwitterionic*) conformer relative to the most stable canonical structure with a single formal charge site (charge solvation; CS) of aliphatic amino acids (e.g., Pro, *N*-methyl alanine, *N*-methyl glycine, and glycine) does not increase with size and polarizability of the alkali metal cations, in contrast to the trend commonly found for functionalized amino acids. In fact, the relative stability of SB over CS conformers reaches a maximum at $[\text{amino acid} + Na]^+$. A uniform SB structure and two characteristic CS conformers are identified by theory to be relevant for alkali metalized Pro, *N*-methyl alanine, and *N*-methyl glycine. For CS structures, the alkali metal cation is either coordinated to the nitrogen and the carbonyl oxygen of the acid functionality (Li^+, Na^+) or is solely interacting with the carboxylic acid oxygens (K^+, Rb^+, Cs^+).

The IRMPD spectra exhibit clearly distinguishable bands for the CO stretching modes of the carboxylic acid moiety in CS structures and for the carboxylate moiety in SB structures, allowing reliable structure assignments for all complexes investigated. The IRMPD spectra clearly exhibit the presence of mixed populations of SB and CS structures with the contribution of CS increasing toward the larger metal cations, in good agreement with the predictions from computational modeling. The special trend regarding formation and stability of individual gas-phase ion structures of aliphatic amino acids, lacking functionalized α-side chains, can be rationalized with the concept of hard and soft Lewis acids and bases. Furthermore, calculations show that the trends with metal cation size found for aliphatic amino acids with secondary amines are similar for ordinary aliphatic amino acids (Gly, Ala).

1. Introduction

The amino acid proline (Pro) is special in many respects. Pro is the only proteinogenic amino acid with a secondary nitrogen in the α-position. The twofold substitution of the amine is the reason for its high gas-phase basicity and proton affinity,[1] which in turn makes Pro a favorable site for protonation in electrospray-MS of peptides and proteins. The high proton affinity makes the *N*-terminal amide bond of Pro particularly sensitive to charge driven fragmentation reactions in collision-induced dissociation (CID) experiments.[2] Utilizing this special feature, Pro is included in new collision-induced dissociative chemical cross-linking reagents to enable selective and preferred cleavage upon low-energy collisional activation.[3,4]

The pyrrolidine ring of Pro restricts its conformational flexibility and strongly influences the secondary structure of proteins.[5,6] The structural rigidity of Pro stabilizes bends in the backbone and holds the *N*- and *C*-terminal end of the protein in place for establishment of the H-bonding network for protein *γ*- and *β*-turns.[7] In addition, poly-proline peptides or proline-rich parts of proteins can adopt unique left-handed P_{II} helix structures,[8,9] which are important in numerous biological functions, such as signal transduction,[10] cell motility,[11] immune response,[12] and perhaps formation of amyloid plaques.[13,14] Additionally, Pro has gained wide recognition as a very effective organocatalyst in asymmetric organic synthesis,[15,16] e.g., as a Lewis base catalyst in “Iminium Catalysis”.[17]

In general, the structure, function, and activity of amino acids, peptides and proteins are strongly determined by the significant electric field resulting from the formation of zwitterionic structures in polar solution.[18] For a microscopic understanding of the structural features of selected ion structures it is reasonable to study isolated amino acid molecular ions or amino acid ion clusters with a limited number of solvent molecules in the gas phase.[19-23] Although gas-phase structures may not be directly related to the situation in solution, gas-phase studies allow the detailed examination of individual characteristics of ions, e.g., intramolecular hydrogen bonding patterns [24] or interactions of molecular residues with counterions.[25]

Photodissociation spectroscopy in the infrared has emerged as a powerful method to directly probe ion structures in the gas phase, for instance to differentiate between salt bridge (SB; *zwitterionic*) conformers and alternative structures with a single formal charge site (*canonical*; charge solvated, CS) of a number of biologically and chemically relevant species.[26-28] Amino acids complexed with alkali[28-34] and alkaline earth metal cations,[35-40] as well as cationized peptides[39,41-44] and proteins [45-46] have been investigated. Many of these photodissociation experiments were conducted in the infrared wavelength range using light generated by a tunable free electron laser (FEL) [47], which is typically scanned between 5 and 20 μm in these experiments.[18,25-32,34-45]

Isolated amino acids are non-zwitterionic in the gas phase, but complexation with metal cations can stabilize zwitterionic forms.[28,48] For instance, both calculations [49] and experiments [50,51] indicate that neutral Pro adopts a canonical conformation in the gas phase. However, in the complex of Pro and Na^+ (Na^+Pro), Pro adopts a zwitterionic structure forming a SB complex, which is more stable than the CS conformer by 12–18 kJ/mol.[23,48,52-55] The gas-phase ion structure of potassiated Pro was recently examined by IRMPD spectroscopy and computational modelling and the results suggest that a mixed population of SB and CS conformers (with a strong preference for the former) is formed in the gas phase.[56] Similarly, McMahon and Wu showed that Pro adopts a zwitterionic structure when complexed with the methylammonium ion $[Pro + (CH_3NH_2)H]^+$.[18] Moision and Armentrout studied the gas-phase ion structure of Pro and its four- and six-membered ring analogues with Li^+, Na^+, and K^+ with threshold CID and computational modeling. They found bond energies most consistent with ground state salt bridge structures in the gas phase.[52] The ion structures of Pro in molecular ions with alkaline earth metal cations Be^{2+}, Mg^{2+}, and Ca^{2+} were theoretically examined and indicate that Pro prefers a CS conformer with Be^{2+} and a SB structure with Mg^{2+} and Ca^{2+} cations.[57]

Many studies of metal cation complexes of α-functionalized amino acids show a trend where the SB form becomes more stable compared to CS forms as the size and/or charge of the metal cation increases,[29,30,35,36,57-59] although the opposite trend was reported for sodiated and rubidiated complexes of glycine and alanine.[60] It is important to note that the formation of stable SB structures in the gas phase is not only determined by the nature of the metal cation, but also depends strongly on the gas-phase basicity of the amino acid.[60,61] On the other hand, in spectroscopic studies of cationized Lys and ε-*N*-methyl lysine, Williams and coworkers demonstrated that the relation between proton affinity and zwitterion stability can only be used as a first estimate, because competing stabilization effects, such as ion solvation and hydrogen bonding, can also contribute.[58,62]

In the present work, the gas-phase ion structures of the aliphatic amino acids having secondary amines, Pro and *N*-methyl Ala, complexed with alkali metal cations are systematically examined by IRMPD spectroscopy and computational modelling. This study continues and extends our preliminary study on the gas-phase ion structure of potassiated proline (K^+Pro).[56] With the use of computational modeling, the conclusions of this study are further expanded to aliphatic amino acids in general, i.e., those having a primary amine function and thus a lower proton affinity but no functionalized side chain.

2. Methods

2.1. Materials

All solvents and chemicals used for the synthetic work were purchased from ABCR (Karlsruhe, Germany) or Acros Organics (Geel, Belgium) and were used without further purification.

N-methyl proline

N-methyl proline was synthesized according to a procedure published by Aurelio et al.[63] Pro was dissolved in methanol and the solution was treated with an aqueous formaldehyde solution (40%) in the presence of 10% palladium on charcoal in a hydrogen atmosphere (1 bar; 16 h; 20 °C). The catalyst was removed by filtration and *N*-methyl proline was isolated as pure solid by removal of the solvent.

N-methyl proline methylester

L-proline was esterified with thionyl chloride in methanol for 16 h at 0 °C. The solvent was removed in vacuum and the residue was taken up in methanol and evaporated twice.[64] For *N*-methylation, the resulting proline methylester hydrochloride was dissolved in methanol and an aqueous formaldehyde solution (40%) was added, followed by the addition of palladium on charcoal (10%). The suspension was stirred in a hydrogen atmosphere (1 bar; 4 h; 20 °C) and filtered over Celite.[63] Removal of the solvent gave an oil, which was dissolved in water and washed with dichloromethane. The aqueous phase was treated with sodium bicarbonate and extracted with dichloromethane thrice. The combined organic layers from the basic extraction were dried over magnesium sulfate and after removal of the solvent under reduced pressure, *N*-methyl-L-proline methylester was isolated as a colorless liquid.

N-methyl alanine

Racemic *N*-methyl alanine (NMA) was purchased from Bachem AG (Bubendorf, Switzerland) and used without further purification.

2.2. Mass Spectrometry and Photodissociation

A 4.7 T Fourier-transform ion cyclotron resonance (FTICR) mass spectrometer was used for the IRMPD experiments and has been described in detail elsewhere.[26,65-67] Tunable radiation for the photodissociation experiments is generated by the free electron laser for infrared experiments (FELIX).[47] For the present experiments, spectra were recorded over the wavelength range from 1000 to 1800 cm^{-1}. Pulse energies were around 50 mJ per macropulse of 5 μs duration, although they fell off to about 20 mJ toward the blue edge of the scan range. The fwhm bandwidth of the laser was typically 0.5% of the central wavelength. The cationized amino acids were formed by electrospray ionization (ESI) using a Micromass Z-Spray source and a solution of 1 mM amino acid and 1 - 2 mM alkali metal chlorides in 95%:5% MeOH/H_2O. Solution flow rates ranged from 15 to 30μL/min and the electrospray needle was generally held at a voltage of +3.2 kV. Ions were accumulated in a hexapole trap for about 2 s before being injected into the ICR cell via an rf octopole ion guide. All complex ions were irradiated for 3 s, corresponding to interaction with 15 macropulses.

IR activation of the Na^+, K^+, Rb^+, and Cs^+ complexes of proline and *N*-methyl alanine leads to the exclusive loss of the neutral amino acid yielding the bare alkali metal cation, which is also observed for potassiated *N*-methyl proline and *N*-methyl-proline methylester (Figure 11S Supporting Information). The recording of the IR spectra of both Na^+Pro and Na^+*N*-methyl alanine was complicated by the low detection efficiency of the sodium product ion channel at *m/z* 23 because of its high ICR frequency (Figure 9 and 2S Supporting Information). IRMPD of the lithiated complex ions of proline and *N*-methyl alanine leads mainly to the loss of [C,2O,2H] ($\Delta m = 46u$) and thereby to the formation of product ions at *m/z* 76 and at *m/z* 64, respectively. The former result agrees with the lowest energy channel observed in TCID experiments.[52] Additionally, IRMPD of [*N*-methyl alanine + Li]$^+$ delivers an ammonium product ion ($[C_3H_8N]^+$) at *m/z* 58 ($\Delta m = 52u$). IRMPD spectra were recorded by monitoring the respective product ions formed over the 1000-1800 cm^{-1} frequency range. The IRMPD yield was determined from the precursor (I_P) intensity and the intensity of the product ion (I_{M+}) after laser irradiation at each frequency:

$$\text{IRMPD yield} = I_{M+} / (I_P + I_{M+}) \qquad (1)$$

The yield was normalized linearly with laser power to roughly account for changes in laser power as a function of photon energy.[24]

2.3. Computational Modeling

For the calculations, various structures of alkali metal cationized amino acids were analyzed with a Mixed Low Mode/Monte Carlo multiple minimum conformational search using MacroModel 8.1 (Schrodinger Inc., Portland, OR). The conformational search was performed in 5000 steps, each followed by minimization using the Merck Molecular Force Field (MMFF94s). Candidate structures with low MMFF energy were selected for higher level calculations.

B3LYP computations use the 6-311++G(2d,2p) basis set on all atoms as implemented in Gaussian 03,[68] except for Rb and Cs, which utilize the Stuttgart-Dresden effective core potential (ECP) basis set SDD.[69,70] Harmonic frequency calculations verify that all structures correspond to local minima on the potential energy surface (PES) and provide zero point energies (ZPE). Frequencies are scaled by a factor of 0.98 as found to be best suited for the level of theory applied.[71] For comparison to experiment, calculated vibrational frequencies are convoluted using a 20 cm^{-1} fwhm Gaussian line shape. B3LYP energies including ZPE corrections of all optimized geometries are presented in Tables 1 and 2. Additional calculations on alkali metalized *N*-methyl glycine and glycine are also conducted, with relative energies of all conformers listed in Tables 1S and 2S in the Supporting information. All gas-phase ion structures are generated with Chemcraft 1.6 and depicted as ball and stick models.[72] Individual gas-phase ion structures are specified according to a nomenclature introduced by Armentrout (Figure 2 and Tables 1, 2 and 1S in the Supporting Information).[52,73,74] The general differentiation between SB and CS structures is followed by the metal cation binding pattern in square brackets (e.g. [N,CO]: bidentate interaction of the metal cation with the amine nitrogen and the carbonyl oxygen) and finally structural characteristics of the amino acid conformation are abbreviated (e.g., C3u: carbon 3 of the pyrrolidine ring points upwards in the same direction as the carboxyl or carboxylate group; tOH indicates that the OCOH carboxylic acid group has a trans orientation, whereas a cis orientation, which has a OH···OC hydrogen bond, is otherwise present).

Transition states for proton transfer between SB and CS structures were located by conducting relaxed potential energy surface scans, in which the expected reaction coordinate is systematically varied while allowing all other degrees of freedom to optimize, at the same level of theory used above. Once located, these transition states were fully optimized with one imaginary frequency.

Results and Discussion

IRMPD spectroscopy of alkali metal cationized proline

IRMPD spectra of Pro with the complete series of alkali metal cations (Li^+, Na^+, K^+, Rb^+, and Cs^+) are shown in Figure 1. The IRMPD spectra were recorded over the wavelength range 1000-1850 cm^{-1} to detect the characteristic CO stretching mode, which is very indicative for the presence of either SB or CS structures. For SB structures, which contain the anionic carboxylate moiety, this vibration is expected in the region between 1650-1700 cm^{-1}, whereas for CS structures, where the carboxylic acid carbonyl is maintained, it should lie between 1700 and 1800 cm^{-1}.[29-32,54,56,75,76]

Figure 1

Selected individual spectra are discussed in relation to calculated spectra below, but Fig. 1 allows one to spot trends in the spectra of all five complexes. Major absorptions are found in the range between 1600-1800 cm^{-1} and 1300-1400 cm^{-1}. Additionally, two minor bands below 1300 cm^{-1} are detected in all spectra except for that of Cs^+Pro. For Li^+Pro and Na^+Pro, the dominant band near 1650 cm^{-1} is accompanied by a weaker shoulder to the red at about 1580 cm^{-1}. In the IRMPD spectrum of potassiated Pro, the main band near 1650 cm^{-1} also exhibits a shoulder to the blue at 1725 cm^{-1}. For Rb^+ and Cs^+ complexes, this additional band at 1735 cm^{-1} gains substantially in intensity, so that it eventually becomes the most intense feature for Cs^+Pro.

As noted in the introduction, Drayss et al. interpretated the IRMPD spectrum of potassiated proline with a mixture of SB and CS structures being present, with the former dominating. This interpretation relies on the fact that a low-intensity band is found in the region of the characteristic CO stretches at 1725 cm^{-1}, which is not predicted for any of the SB structures of K^+Pro.[56] The computed spectra of the lowest energy CS conformer CS[COOH]C3u and its distorted-ring isomer CS[COOH]C3d (Figure 2) show a band at 1735 cm^{-1}. Hence, this band at the blue end of the spectrum suggests the presence of a minor fraction of CS conformers, despite the significant energy gap of more than 15 kJ mol^{-1} predicted by both DFT and MP2 calculations,[56] as well as previous work at similar levels of theory providing differences of 10 - 18 kJ/mol.[52] No other bands characteristic for the CS conformers can be identified definitively because they coincide with absorption bands of the prevalent SB structures. All relevant SB and CS structures of K^+Pro identified by theory are shown in Figures 2 and 5S in the Supporting Information. Corresponding DFT energies are given in Table 1. Note that each isomer exists as a conformer pair differing only in the orientation of the five-membered pyrrolidine ring (Figure 2).[48,54,56]

Figure 2

Figure 3

Table 1. Relative energies including ZPE corrections [kJ mol^{-1}] of all conformers as predicted by B3LYP/6-311++G(2d,2p) theory for the alkali metalized proline precursor ions M$^+$Pro with M$^+$ = Li$^+$, Na$^+$, K$^+$, Rb$^+$, and Cs$^+$.

	Li$^+$Pro	Na$^+$Pro	K$^+$Pro	Rb$^+$Pro	Cs$^+$Pro
SB[CO$_2^-$]C3u	0.0	0.0	0.0	0.0	0.0
SB[CO$_2^-$]C3d	1.7	2.2	2.7	3.1	3.4
CS[COOH]C3u	→SB[CO$_2^-$]*	26.5	14.5	5.9	1.8
CS[COOH]C3d	42.9	28.3	16.2	7.6	2.9
CS[N,CO]C3u	11.0	23.0	25.5	23.0	21.5
CS[N,CO]C3d	7.6	19.1	21.6	19.3	17.9
CS[N,CO]NHu	33.6	36.9	35.3	30.6	28.0
CS[N,CO]C3u,tOH	32.7	44.5	45.5	42.4	40.0
CS[N,CO]C3d,tOH	29.5	41.0	42.3	39.2	37.2
CS[COOH]NHu	80.0	65.5	50.7	40.0	33.8
CS[N,OH]C3u	52.3	61.1	60.9	58.7	53.1
CS[N,OH]C3d	50.1	59.7	59.5	54.9	52.1
CS[N,OH]NHu	67.1	67.4	63.9	57.5	53.9
Transition states	-	21.8	12.2	6.6	4.0

*Potential energy surface scanning shows that the CS[COOH]C3u conformer collapses into the SB[CO$_2^-$]C3u conformer due to the absence of a transition state between the two structures.

IRMPD spectroscopy of potassiated proline, N-methyl proline, and N-methyl proline methylester

To further elucidate the structure assignment of K$^+$Pro, we examined the spectra of two related systems that serve as benchmarks for either a charge-solvated structure or a salt-bridge structure. Because of its increased basicity as compared to that of Pro, *N*-methyl proline forms a purely salt-bridge structure upon complexation with K$^+$.[24,34,60,61] On the other hand, the *N*-methyl proline methylester has no acidic proton and can thus only form charge-solvated structures. The spectra of the three potassiated complexes are overlaid in Figure 3. Potassiated *N*-methyl proline exhibits a single and well resolved absorption at 1660 cm^{-1}, which corresponds to the carboxylate anti-symmetric OCO stretch mode of the SB[CO$_2^-$]C3d structure, as evidenced by comparison to the calculated spectrum in Figure 4.[24] The blue-shifted shoulder as observed for K$^+$Pro is clearly absent here. In contrast, the only band in the 1600-1800 cm^{-1} range in the spectrum of the potassiated *N*-methyl proline methylester, which can only adopt a CS structure, is blue-shifted to about 1725 cm^{-1} and must result from a carboxylic acid CO stretch mode. This band coincides nicely with the blue shoulder in the spectrum of K$^+$Pro. Hence, the spectra of the two reference compounds provide independent evidence for a mixture of CS and SB structures in K$^+$Pro (see also Figure 4S of K$^+$Pro in the Supporting Information).

Upon further analysis of the spectra in Figure 3, one notices large differences in the 1000 - 1300 cm^{-1} range between the spectra of potassiated Pro and *N*-methyl proline on the one hand and the potassiated *N*-methyl proline methylester on the other hand. In the former species, the weak bands correspond to delocalized vibrations of the pyrolidine ring, whereas in the ester, the enhanced activity results from the intense C-O-C vibrations of the ester linkage, which couple partly to the pyrolidine ring vibrations (Figure 12S in the Supporting Information). The weak 1600 cm^{-1} shoulder on the red side of the CO stretch in the spectra of K$^+$Pro and K$^+$NMePro is not explained by theory (see Figures 3 and 4) and we assume that they can be attributed to an overtone or combination mode of the salt bridge structure.

Figure 4

IRMPD spectroscopy of lithiated proline

The IRMPD spectrum of lithiated Pro exhibits an unresolved composite band with a minor contribution at 1580 cm^{-1} and a major absorption around 1655 cm^{-1} (see Figure 5). Additionally, four resolved bands are observed at 1410, 1310, 1220 and 1160 cm^{-1}, listed in order of decreasing intensity. In the 1150 and 1450 cm^{-1} region, the experimental spectrum agrees favorably with that calculated for the SB[CO_2^-]C3u structure, which was found to be the most stable conformer for Li$^+$Pro (see Figure 5, Table 1, Figure 1S Supporting Information). As the computed IR spectra of the nearly iso-energetic conformer pairs SB[CO_2^-]C3u and SB[CO_2^-]C3d are almost identical (an observation that is common to all metal cations as well as the other amino acids discussed below), they cannot be distinguished experimentally and only one of them is displayed in Figure 5.[56] Given the intensity observed near 1180 and 1440 cm^{-1} and the blue tail on the main CO stretching band, a minor contribution of the CS[N,CO]C3d conformer cannot be ruled out completely; however, it appears unlikely that any CS is present from the trends seen in the spectra of the entire M$^+$Pro series in Figure 1, *i.e.*, a distinct blue shoulder starts to appear only at the complex with K$^+$. Again, a weak shoulder is observed near 1580 cm^{-1}, which is not predicted by theory for SB[CO_2^-]C3u and which we suggest corresponds to an overtone or combination mode of SB structures. Figure 1 shows that this shoulder gradually disappears for complexes with larger cations, which have a decreasing fraction of SB structures (*vide infra*), thus consistent with this mode appearing only in the SB structures in Figure 3.

Figure 5

As Table 1 illustrates, the most stable CS conformer of Li$^+$Pro (CS[N,CO]C3d) differs from the most stable CS structure found for K$^+$Pro (CS[COOH]C3u in Figure 2). Computations identify two types of low-lying CS structures for M$^+$Pro complexes (see Table 1). For the smallest alkali metal cations, lithium and sodium, the preferred CS structure of the complex shows a bidentate binding pattern, in which the metal cation is chelated by the carbonyl oxygen atom of the carboxylic acid moiety and the amine nitrogen atom (CS[N,CO]), whereas the larger metal cations, K$^+$, Rb$^+$, and Cs$^+$, preferably adopt a conformer in which the metal cation is solely interacting with the carboxylic acid group (CS[COOH]). The amine nitrogen is hydrogen bonded to the acidic proton in these structures (see Figure 2). An analogous competition of CS structures varying with the alkali metal cation, was found for serine,[29] threonine,[30] asparagine,[31] methionine,[32] cysteine,[33], and tryptophan.[71]

This finding is consistent with the bidentate CS structures of Gly with sodium and potassium, which were studied in detail by Moison and Armentrout.[73,74] The dissection of the alkali metal cation-Gly interactions into individual contributions showed that Na$^+$ binds most strongly to the carbonyl oxygen and then prefers binding to the amine group rather than to the hydroxyl group leading to the CS[N,CO] conformer. K^+, on the other hand, binds less tightly to the amine group but more strongly to the acid hydroxyl group leading to the formation of a stable CS[COOH] conformer. Therefore, the strength of alkali metal cation binding in bidentate chelation patterns depends not only on the intrinsic binding affinity of the functional groups involved but also on how much conformational mobility the ligand has to facilitate.[73,74]

IRMPD spectroscopy of cesiated proline

The IRMPD spectrum of cesiated Pro exhibits an unresolved composite band from 1300 to 1500 cm^{-1} and a major absorption spanning from 1660 to 1800 cm^{-1}. Especially, the broadness and the nearly flat top band shape of this absorption suggest the simultaneous presence of both the SB[CO_2^-]C3u structure and the most stable CS conformer CS[COOH]C3u (see Table 1, Figure 6, Figure 9S and 10S in the Supporting Information). The prominent CO stretching modes of both the carboxylate group of the SB[CO_2^-]C3u structure, which is calculated somewhat red shifted at 1675 cm^{-1}, and of the carboxylic acid moiety of the CS[COOH]C3u conformer (calculated at 1740 cm^{-1}), match the broad feature observed around 1660-1800 cm^{-1}. The shape of this strong absorption band thus suggests a mixed population of CS and SB conformers. However, the predicted single-photon IR intensities of these two features are 500 km mol^{-1} for the C=O stretching mode of CS versus 300 km mol^{-1} for the OCO asymmetric stretch of SB. Equal intensities of the two bands in the experimental spectrum would thus suggest a higher abundance of SB[CO_2^-]C3u over CS[COOH]C3u (although observed intensities in an IRMPD spectrum may not be quantitative). However, theory finds the SB[CO_2^-]C3u and CS[COOH]C3u conformers of Cs^+Pro to be virtually equally stable (see Table 1). Further evidence for a mixture of these structures is provided by the good agreement of the broad experimental band spanning from 1370 to 1500 cm^{-1}, which likely results from a combination of the NH bending modes calculated at 1400-1450 cm^{-1} for CS[COOH]C3u and the NH bending and CC stretching modes of SB[CO_2^-]C3u found at 1300-1400 cm^{-1}.

Figure 6

Inspecting the calculations for the entire M^+Pro series, one notices that the stability of the SB conformer relative to the stability of the most stable CS structure of Pro is not increasing with size and polarizability of the alkali metal cations (Table 1), in contrast to the trend that is commonly found for functionalized amino acids (see Figure 7).[29,30,35,57-59] In fact, the relative stability of SB over CS conformers for M^+Pro reaches a maximum for Na^+Pro and decreases for larger alkali metal cations. The experimental IRMPD spectra of M^+Pro complexes indeed confirm this trend and are generally consistent with the predictions from computational modelling. Below we show that this trend is generally observed for aliphatic amino acids with a secondary amine. In addition, although aliphatic amino acids with a primary amine always have a ground state CS structure, the computed trend with metal cation size is analogous.

Figure 7

Transition states between CS[COOH] and SB[CO_2^-] conformers of proline

As indicated in Table 1, the CS[COOH]C3u structure for Li^+Pro is not stable and collapses to the SB[CO_2^-]C3u structure. The relaxed potential energy surface scan of the proton motion from the SB towards the putative CS structure shows an inflection point at an appropriate geometry, but verifies that there is no minimum. For Na^+Pro, the CS structure is stable (by 1.7 kJ/mol) but is found to have a higher energy than the transition state (TS) once zero point energies are included because the imaginary frequency (i700 cm^{-1}) is no longer included. Therefore, along the 0 K surface, the CS structure for Na^+Pro will also collapse to the SB structure. A similar situation occurs for K^+Pro where the CS[COOH] structure is more stable than the TS (i953 cm^{-1}) by 5.2 kJ mol^{-1} before ZPE corrections but less stable by 2.4 kJ mol^{-1} after (Table 1). For Rb^+Pro and Cs^+Pro, the well associated with the CS structures is now sufficiently deep that a true TS lies along the 0 K surface, although the TSs lie only 0.6 and 2.2 kJ mol^{-1} above the CS structures, respectively.

Given these theoretical observations, especially for K^+Pro, it becomes important to understand why the experimental results clearly show the presence of the CS structure. As discussed for the similar situation with metal cationized serine,[29] we believe that it is important to realize that the CS[COOH]C3u and SB[CO_2^-]C3u structures actually reside in the same asymmetric potential well associated with the proton motion between the OH···N and O···HN positions. Because this is a proton motion, the harmonic vibrational frequencies calculated are fairly high, ranging from 2750 – 3150 cm^{-1}. Thus, the zero point energy in this mode is 16 – 19 kJ mol^{-1}, sufficiently high that for the heavier metal cations, the zero point level lies *above* the TS barrier height, Table 1. (However, it should be realized that because of the asymmetry of the potential well such harmonic frequencies are unlikely to be accurate.) Thus, the wavefunction associated with these species contains intensity in both wells such that the IRMPD probe (in orthogonal vibrations) is capable of observing both species.

IRMPD spectroscopy of alkali metal cationized N-methyl alanine

To further probe the influence of non-polar residues on the formation of distinct ion structures in the gas phase, the amino acid alanine (Ala) with its methyl group in the α-position serves as a grossly simplified model functionality for the pyrrolidine ring of Pro.[77] To mimic the gas-phase basicity of the secondary amine functionality of Pro, *N*-methylated alanine was studied. The IRMPD spectra of *N*-methyl alanine with the series of alkali metal cations are shown in Figure 8.

Figure 8

In the spectra of lithiated and sodiated *N*-methyl alanine, a major band is found around 1600-1700 cm^{-1}. In the IRMPD spectrum of potassiated *N*-methyl alanine, the band around 1670 cm^{-1} exhibits a shoulder near 1730 cm^{-1}. This shoulder becomes substantially more intense in the spectra of the complexes with the larger alkali metal cations, Rb^+ and Cs^+. This trend is similar to that described above for the alkali metal cation complexes with Pro. In addition, the IRMPD spectra of alkali metalized *N*-methyl alanine exhibit a characteristic absorption in the 1300 - 1500 cm^{-1} range. For the complexes with K^+, Rb^+ and Cs^+, this feature is accompanied by a minor band near 1450 cm^{-1}, which appears to be unresolved for the Li^+ complex. For sodiated *N*-methyl alanine, a substantially narrower band is observed in this range. The spectra of selected complexes are discussed in more detail below.

IRMPD spectroscopy of sodiated N-methyl alanine

The IRMPD spectrum of sodiated *N*-methyl alanine displays two major absorptions in the ranges 1280 - 1420 cm^{-1} and 1570 - 1650 cm^{-1} (Figure 9). The latter band appears to be composed of two unresolved sub-bands in agreement with the doublet including the carboxylate CO stretching mode calculated for the most stable SB structure. The other rather unresolved band ranging from 1280 to 1420 cm^{-1} is also in reasonable agreement with the computed spectrum of the SB[CO_2^-]e conformer (Figure 9). The very weak absorption near 1665 cm^{-1} is the only hint for the presence of a small fraction of CS conformers. The dominant preference for the formation of a SB structure of sodiated *N*-methyl alanine is consistent with theory, as the most stable CS[N,CO]e conformer is predicted to be less stable than the SB structure by 16.0 kJmol^{-1} (Table 2, Figure 9, Figure 15S in the Supporting Information). This result further supports the trend found for alkali metalized Pro, where the relative stability of SB versus CS conformers also reaches a maximum for the complex with Na$^+$ (see Figure 7).

Figure 9

Table 2. Relative energies including ZPE corrections [kJ mol^{-1}] for all conformers of alkali metal ion complexes of *N*-methyl alanine (M$^+$NMA) with M$^+$ = Li$^+$, Na$^+$, K$^+$, Rb$^+$, and Cs$^+$ as predicted by B3LYP/6-311++G(2d,2p) calculations.

	Li$^+$NMA	Na$^+$NMA	K$^+$NMA	Rb$^+$NMA	Cs$^+$NMA
SB[CO_2^-]e	0.0	0.0	0.0	0.0	1.8
SB[CO_2^-]z	7.9	8.5	8.6	8.4	10.2
CS[COOH]e	36.8	23.4	11.7	3.4	0.0
CS[COOH]z	45.1	31.5	19.4	11.3	7.8
CS[N,CO]e	6.7	16.0	17.1	13.8	13.6
CS[N,CO]z	16.6	25.3	25.9	24.8	24.6
CS[N,CO]OHd,e	29.0	37.6	37.2	33.3	32.2
CS[N,CO]OHd,z	38.5	46.9	48.4	44.7	44.0
CS[N,OH]e	47.9	53.7	52.5	46.7	45.3
CS[N,OH]z	54.0	60.2	58.4	52.8	51.4
Transition states	33.0	18.8	9.5	4.0	3.3

IRMPD-spectroscopy of rubidiated N-methyl alanine

The IRMPD spectrum of rubidiated *N*-methyl alanine also displays a doublet-like structure in the CO-stretching range (Figure 8). However, the bands are substantially blue-shifted compared to the feature in the Na$^+$ complex. Comparison of the IRMPD spectrum with the computed spectra of the two most stable gas-phase conformers, i.e., SB[CO_2^-]e and CS[COOH]e, which is only 3.4 kJmol^{-1} higher in energy, is presented in Figure 19S in the Supporting Information. The partially resolved doublet shape of the band at 1600 - 1700 cm^{-1} is in good agreement with the calculated CO stretches of both the SB[CO_2^-]e and CS[COOH]e structures, suggesting that both conformers are simultaneously present. An estimate of the relative abundances of the two conformers on the basis of predicted intensities is only roughly possible as pointed out for Cs$^+$Pro. The predicted intensities of the two CO stretching modes are similar to those in Cs^+Pro (500 km mol^{-1} for CS, 300 km mol^{-1} for SB), suggesting a higher abundance for SB than for CS.

IRMPD spectroscopy of cesiated N-methyl alanine

The IRMPD spectrum of cesiated *N*-methyl alanine is shown in Figure 10 and the comparison with the computed spectra of the nearly isoenergetic SB[CO_2^-]e (+1.8 $kJmol^{-1}$) and CS[COOH]e conformers suggests again a mixture of these structures (Figure 20S in the Supporting Information). Keeping the somewhat qualitative character of the correlation between relative band intensities and ion abundances in mind, the two bands making up the doublet feature suggest that the CS conformer is now further stabilized with respect to the SB conformer, again in good agreement with the computed energetics (Table 2).

Figure 10

Discussion of transition states between CS[COOH] and SB[CO_2^-] conformers of N-methyl alanine

As in the case of Pro, we examined the transition states between the CS[COOH]e and SB[CO_2^-]e structures (Table 2). Here, the TSs for the Li^+, Na^+, and K^+ systems again lie below the energy of the CS structure once ZPE corrections are included, whereas there remain distinct potential wells for the CS structures of the Rb^+ and Cs^+ systems. Again the latter are quite shallow at only 0.6 and 3.3 kJ mol^{-1}, respectively, and in the Cs^+ case, the TS lies only 1.5 kJ mol^{-1} above the SB structure. Here the calculated harmonic vibrational frequencies of these proton motions vary from 2800 – 3225 cm^{-1}, such that their zero point energy is again 16 – 19 kJ mol^{-1}. As for the Pro systems, there must exist an asymmetric potential well for this proton motion that allows the wavefunction to simultaneously populate both structures here.

General trends and concluding remarks

The structure of alkali metal cation complexes of the secondary amino acids Pro and *N*-methyl alanine are investigated. Both aliphatic amino acid complexes are shown to possess analogous gas-phase structures and moreover, the relative stabilities of CS versus SB structures as a function of metal cation size are similar (Figure 7). Note that the two molecules were specifically selected because of their high gas-phase basicity resulting from the secondary amine, which stabilizes the SB conformers sufficiently that small changes in metal cation binding can alter the structure from one conformer to another.[58] In contrast to several amino acid metal cation binding studies reported recently, the amino acids studied here do not possess a heteroatom or aromatic functionality in their α-side chain and interaction with the metal cation occurs exclusively through the C- and N-termini. Computations predict similar SB and CS structures for Pro and *N*-methyl alanine, where only one low-energy SB[CO_2^-] structure is found, whereas two bidentate CS conformers are competing for highest stability. For lithiated and sodiated molecular ions, the metal cation is coordinated to the amine nitrogen and the carbonyl oxygen of the carboxylic acid functionality (CS[N,CO]). From potassium onwards (K^+, Rb^+, and Cs^+), the most stable CS structure is CS[COOH], in which the metal cation is solely interacting with the carboxylic acid functionality and the amine nitrogen is hydrogen bonded to the acidic proton. Diagnostic bands in the IRMPD spectra are mainly the CO stretching mode of the carboxylate and carboxylic acid moieties for SB and CS conformers, respectively. These modes allow reliable structure assignments for all complexes investigated.

The IRMPD spectra show that SB and CS structures co-exist in all potassiated, rubidiated, and cesiated complexes and that their relative abundances vary significantly with metal cation size. It is the trend in this variation that sets these aliphatic amino acids apart from the functionalized amino acids (see Figure 7), many of which have been spectroscopically investigated recently [29-31,34,58,59,71]. Whereas the functionalized amino acids without exception show an increasing stability of the SB conformer with metal cation size, we find exactly the opposite trend for the aliphatic amino acids, i.e., the CS conformer becomes increasingly more stable relative to SB as the alkali metal cation increases from Na^+ to Cs^+. Although DFT calculations correctly predict these opposite trends, we ask ourselves the intriguing question of what are the physical factors underlying these different trends.

The trend of increasing stability of the CS structure with increasing metal cation size from Na^+ to Cs^+ as observed here for the aliphatic amino acids may straightforwardly be related to the trend in the polarizing effect that the metal cations have on the attached ligands. The larger polarizing effect of the smaller metal cations induces more polarization in the organic ligands, culminating in charge separation for the most polarizing metal cations. Charge-separated SB structures are thus more favorable for small metal cations, and as the polarizing effect decreases toward larger cations, the SB conformer becomes less favorable, thus increasing the relative stability of CS conformers.

This trend can also be explained using the concept of Hard and Soft Lewis Acids and Bases (HSAB) introduced by Pearson,[78,79] which has proven to be very useful to explain the formation of stable Lewis-acid-base complexes. The stability of these complexes is favored for *hard-hard* and *soft-soft* interactions of respective Lewis acids and bases. Here, the small and strongly polarizing metal cations Li^+ and Na^+ can be termed *hard*, whereas the polarizable cations K^+, Rb^+ and Cs^+ are of increasingly softer character. The chelating sites of the aliphatic amino acids are limited to the carboxylic acid and the amine functionality. In the HSAB sense, the negatively charged carboxylate moiety can be considered as being somewhat harder than the uncharged and thus less polarizing conjugate acid functionality in CS structures. Within this framework, the trend of increasing stability of the CS structure with increasing metal cation size can be understood.

Finally, we note that the complexes of Pro and *N*-methyl alanine with Li^+ do not follow the trend explained above and appear to be the exception in Figure 7. We believe this may be a result of the extensive distortion that the very small lithium cation exerts on these ligands, such that the trends are not the same as for the larger, less perturbative alkali metal cations. Such distortions also mean that theory is less reliable, as discussed elsewhere.[80]

In contrast to the aliphatic amino acids, the functionalized amino acids have in common that they possess either a hetero-atom (N,O,S) or an aromatic ring in their side chain. These functionalities are all Lewis basic and can donate electron density to the metal cation thus solvating the charge. It is thus expected that the presence of an additional Lewis basic site in these amino acids provides an increased stability to CS structures (although for particularly basic side chains, such as in Arg, internal proton transfer forming an SB structure may be preferred). Stabilization by charge solvation relies on an effective shielding of the formal charge site from the vacuum. As the amino acids are relatively small ligands, this shielding becomes less effective as the ionic radius of the metal cation increases, leaving the charge increasingly exposed to the vacuum. Hence, the CS structure becomes less stable with increasing metal cation size, thereby increasing the relative stability of the SB conformer.

We conclude that the observation of opposite structural trends with metal cation size for aliphatic versus functionalized amino acids is the result of two different effects that act in opposite directions. On the one hand, the polarizing effect of the metal cations tends to increase the SB stability as the metal cation gets smaller, while on the other hand smaller cations are sterically more efficiently solvated by the Lewis basic sites available in the amino acid. The latter effect dominates in the amino acids with a functionalized side chain, whereas the former effect dominates for the aliphatic amino acids, which have fewer Lewis basic sites.

The results presented here clearly suggest that the opposite trends observed relate to the aliphatic or non-aliphatic nature of the amino acid side chain. We believe that the trend observed here for the secondary amine aliphatic amino acids Pro and *N*-methyl alanine are generally valid for all aliphatic amino acids, including those having a primary amine (Gly, Ala, Val, Leu, Ile). However, because of their lower basicity, a charge solvation structure is more stable than a salt bridge structure in these amino acids regardless of the alkali metal cation and experimental studies have indeed only identified CS structures.[54,60,73,74] Nonetheless, the trend in relative stability of CS and SB structures is analogous, as is indicated by computations for the series of M^+Gly complexes included in Figure 7, where the curve for M^+Gly is similar to that for the *N*-alkylated species but shifted downwards towards CS (see also Table 2S).

Acknowledgments

Financial support by the “Nederlandse Organisatie voor Wetenschappelijk Onderzoek” and the German Research Foundation (DFG) are acknowledged. PBA acknowledges support from the National Science Foundation (CHE-0748790). MS and MKD thank Frank Dreiocker, Department of Chemistry, University of Cologne, for preparation of the amino acid derivatives and Dr. Dirk Blunk, Department of Chemistry, University of Cologne, for kind assistance with the molecular modeling computations. Generous provision of computing power at the Regional Computing Centre RRZK, Cologne, Germany, in the frame of the D-GRID initiative, and at the Center for High Performance Computing in the University of Utah is gratefully acknowledged. The authors thank Dr. Britta Redlich and Dr. J.D. Steill for skillful assistance at the FELIX facility.

References

[1] A.G. Harrison, The Gas-Phase Basicities and Proton Affinities of Amino Acids and peptides, Mass Spectrom. Rev. 16 (1997) 210-217.

[2] B. Paizs, S. Suhai, Fragmentation Pathways of Protonated Peptides, Mass Spectrom. Rev. 24 (2005) 508-548.

[3] E.J. Soderblom, M.B. Goshe, Collision-Induced Dissociative Chemical Cross-Linking Reagents and Methodology: Applications to Protein Structural Characterization Using Tandem Mass Spectrometry Analysis, Anal. Chem. 78 (2006) 8059-8068.

[4] F. Dreiocker, M.Q. Müller, A. Sinz, M. Schäfer, Collision-induced dissociative chemical cross-linking reagent for protein structure characterization: applied Edman chemistry in the gas phase, J. Mass Spectrom. 2010, DOI: 10.1002/jms.1702

[5] I. Compagnon, J. Oomens, G. Meijer, G. von Helden, Mid-infrared Spectroscopy of Protected Peptides in the Gas Phase: A Probe of the Backbone Conformation, J. Am. Chem. Soc. 128 (2006) 3592-3597.

[6] J. Venkatraman, S.C. Shankaramma, P. Balaram, Design of Folded Peptides, Chem. Rev. 101 (2001) 3131-3152.

[7] E. Vass, M. Hollói, F. Besson, R. Buchet, Vibrational Spectroscopic Detection of Beta- and Gamma-Turns in Synthetic and Natural Peptides and Proteins, Chem. Rev. 103 (2003) 1917-1954.

[8] B.W. Chellgren, T.P. Creamer, Short Sequences of Non-Proline Residues Can Adopt the Polyproline II Helical Conformation, Biochemistry 43 (2004) 5864-5869.

[9] N. Sreerama, R.W. Woody, Poly(Pro)II Helices in Globular Proteins: Identification and Circular Dichroic Analysis, Biochemistry 33 (1994) 10022-10025.

[10] B.K. Kay, M.P. Williamson, M. Sudol, The importance of being proline: the interaction of proline-rich motifs in signaling proteins with their cognate domains, FASEB J. 14 (2000) 231-241.

[11] N.M. Mahoney, P.A. Janmey, S.C. Almo, Structure of the profilin-poly-L-proline complex involved in morphogenesis and cytoskeletal regulation, Nat. Struct. Biol. 4 (1997) 953-960.

[12] T.S. Jardetzky, J.H. Brown, J.C. Gorga, L.J. Stern, R.G. Urban, J.L. Strominger, D.C. Wiley, Crystallographic analysis of endogenous peptides associated with HLA-DR1 suggests a common polyproline II-like conformation for bound peptides, Proc. Natl. Acad. Sci. U.S.A. 93 (1996) 734-738.

[13] E.W. Blanch, L.A. Morozova-Roche, D. A.E. Cochran, A.J. Doig, L. Hecht, L.D. Barron, Is polyproline II helix the killer conformation? A Raman optical activity study of the amyloidogenic prefibrillar intermediate of human lysozyme, J. Mol. Biol. 301 (2000) 553-563.

[14] J. Jarvet, P. Damberg, J. Danielsson, I. Johansson, L.E.G. Eriksson, A. Gräslund, A left-handed 3_1 helical conformation in the Alzheimer $A\beta$(12-28) peptide, FEBS Lett. 555 (2003) 371-374.

[15] A.G. Doyle, E.N. Jacobsen, Small-Molecule H-Bond Donors in Asymmetric Catalysis, Chem. Rev. 107 (2007) 5713-5743.

[16] S. Mukherjee, J. Woon Yang, S. Hoffmann, B. List, Asymmetric Enamine Catalysis, Chem. Rev. 107 (2007) 5471-5569.

[17] A. Erkkilä, I. Majander, P.M. Pihko, Iminium Catalysis, Chem. Rev. 107 (2007) 5416-5470.

[18] R. Wu, T.B. Mc Mahon, Stabilization of the Zwitterionic Structure of Proline by an Alkylammonium Ion in the Gas Phase, Angew. Chem. 119 (2007) 3742-3745.

[19] A.S. Lemoff, M.F. Bush, J.T. O'Brien, E.R. Williams, Structures of Lithiated Lysine and Structural Analogues in the Gas Phase: Effects of Water and Proton Affinity on Zwitterionic Stability, J. Phys. Chem. A 110 (2006) 8433-8442.

[20] M.F. Bush, J.S. Prell, R.J. Saykally, E.R. Williams, One Water Molecule Stabilizes the Cationized Arginine Zwitterion, J. Am. Chem. Soc. 129 (2007) 13544-13553.

[21] R.A. Jockusch, A.S. Lemoff, E.R. Williams, Hydration of Valine-Cation Complexes in the Gas Phase: On the Number of Water Molecules Necessary to Form a Zwitterion, J. Phys. Chem. A 105 (2001) 10929-10942.

[22] S.J. Ye, R.M. Moision, P.B. Armentrout, Sequential Bond Energies of Water to Sodium Glycine Cation, Int. J. Mass Spectrom. 240 (2005) 233–248.

[23] S.J. Ye, R.M. Moision, P.B. Armentrout, Sequential bond energies of water to sodium proline cation, Int. J. Mass Spectrom. 253 (2006) 288-304.

[24] M.K. Drayß, D. Blunk, J. Oomens, B. Gao, T. Wyttenbach, M.T. Bowers, M. Schäfer, Systematic study of the structures of potassiated tertiary amino acids: Salt bridge structures dominate, J. Phys. Chem. A 113 (2009) 9543-9550.

[25] M.F. Bush, J. Oomens, E.R. Williams, Proton Affinity and Zwitterion Stability: New Results from Infrared Spectroscopy and Theory of Cationized Lysine and Analogues in the Gas Phase, J. Phys. Chem. A 113 (2009) 431-438.

[26] J. Oomens, B.G. Sartakov, G. Meijer, G. von Helden, Gas-phase infrared multiple photon dissociation spectroscopy of mass-selected molecular ions, Int. J. Mass Spectrom. 254 (2006) 1-19.

[27] L. MacAleese, P. Maître, Infrared Spectroscopy of Organometallic Ions in the Gas Phase: From Model to Real World Complexes, Mass Spectrom. Rev. 26 (2007) 583-605.

[28] N.C. Polfer, J. Oomens, Vibrational Spectroscopy of Bare and Solvated Ionic Complexes of Biological Relevance, Mass Spectrom. Rev. 28 (2009) 468-494.

[29] P.B. Armentrout, M.T. Rodgers, J. Oomens, J. D. Steill, Infrared Multiphoton Dissociation Spectroscopy of Cationized Serine: Effects of Alkali-Metal Cation Size on Gas-Phase Conformation, *J. Phys. Chem. A*, 112 (2008) 2248-2257.

[30] M.T. Rodgers, P.B. Armentrout, J. Oomens, J.D. Steill, Infrared Multiphoton Dissociation Spectroscopy of Cationized Threonine: Effects of Alkali-Metal Cation Size on Gas-Phase Conformation, J. Phys. Chem. A 112 (2008) 2258-2267.

[31] A.L. Heaton, V.N. Bowman, J. Oomens, J.D. Steill, P.B. Armentrout, Infrared Multiphoton Dissociation Spectroscopy of Cationized Asparagine: Effects of Alkali-Metal Cation Size on Gas-Phase Conformation, J. Phys. Chem. A 113 (2009) 5519-5530.

[32] D.R. Carl, T.E. Cooper, J. Oomens, J.D. Steill, P.B. Armentrout, Infrared Multiple Photon Dissociation Spectroscopy of Cationized Methionine: Effects of Alkali-Metal Cation Size on Gas-Phase Conformation, Phys. Chem. Chem. Phys. (2010) in press.

[33] P. B. Armentrout, E.I. Armentrout, A.A. Clark, T.E. Cooper, E.M.S. Stennett, D.R. Carl, An Experimental and Theoretical Study of Alkali Metal Cation Interactions with Cysteine, J. Phys. Chem. B (2010) accepted for publication.

[34] M.W. Forbes, M.F. Bush, N.C. Polfer, J. Oomens, R.C. Dunbar, E.A. Williams, R.A. Jockusch, Infrared Spectroscopy of Arginine Cation Complexes: Direct Observation of Gas-Phase Zwitterions, J. Phys. Chem. A 111 (2007) 11759-11770.

[35] M.F. Bush, J. Oomens, R.J. Saykally, E.R. Williams, Effects of Alkaline Earth Metal Ion Complexation on Amino Acid Zwitterion Stability: Results from Infrared Action Spectroscopy, J. Am. Chem. Soc. 130 (2008) 6463-6471.

[36] R.C. Dunbar, N.C. Polfer, J. Oomens, Gas-phase Zwitterion Stabilization by a Metal Dikation, J. Am. Chem. Soc. 129 (2007) 14562-14563.

[37] R.C. Dunbar, J.D. Steill, N.C. Polfer, J. Oomens, Dimeric Complexes of Tryptophan with M^{2+} Metal Ions, J. Phys. Chem. A 113 (2009) 845-851.

[38] R.C. Dunbar, A.C. Hopkinson, J. Oomens, C.-K. Siu, K.W. M. Siu, J.D. Steill, U.H. Verkerk, J. Zhao, Conformation Switching in Gas-Phase Complexes of Histidine with Alkaline Earth Ions, J. Phys. Chem. B 113 (2009) 10403-10408.

[39] R.C. Dunbar, J.D. Steill, N.C. Polfer, J. Oomens, Peptide Length, Steric Effects, and Ion Solvation Govern Zwitterion Stabilization in Barium-Chelated Di- and Tripeptides, J. Phys. Chem. B 113 (2009) 10552-10554.

[40] J.T. O'Brien, J.S. Prell, J.D. Steill, J. Oomens, E.R. Williams, Interactions of Mono- and Divalent Metal Ions with Aspartic and Glutamic Acid Investigated with IR Photodissociation Spectroscopy and Theory, J. Phys. Chem. A 112 (2008) 10823-10830.

[41] J.S. Prell, M. Demireva, J. Oomens, E.R. Williams, Role of Sequence in Salt-Bridge Formation for Alkali Metal Cationized GlyArg and ArgGly Investigated with IRMPD Spectroscopy and Theory, J. Am. Chem. Soc. 131 (2009) 1232-1242.

[42] B. Lucas, G.Grégoire, J. Lemaire, P. Maître, F. Glotin, J.P. Schermann, C. Desfrançois, Infrared multiphoton dissociation spectroscopy of protonated *N*-acetyl-alanine and alanyl-histidine, Int. J. Mass Spectrom. 243 (2005) 105-113.

[43] R. Wu, T.B. McMahon, Infrared Multiple Photon Dissociation Spectroscopy as Structural Confirmation for $GlyGlyGlyH^+$ and $AlaAlaAlaH^+$ in the Gas Phase.

Evidence for Amide Oxygen as the Protonation Site, J. Am. Chem. Soc. 129 (2007) 11312-11313.

[44] J.S. Prell, J.T. O'Brien, J.D. Steill, J. Oomens, E.R. Williams, Structures of Protonated Dipeptides: The Role of Arginine in Stabilizing Salt Bridges J. Am. Chem. Soc. 131 (2009) 11442-11449.

[45] J. Oomens, N. Polfer, D.T. Moore, L. van der Meer, A.G. Marshall, J.R. Eyler, G. Meijer, G. von Helden, Charge-state resolved mid-infrared spectroscopy of a gas-phase protein, Phys. Chem. Chem. Phys. 7 (2005) 1345-1348.

[46] Oh, K. Breuker, S.K. Sze, Y. Ge, B.K. Carpenter, F.W. McLafferty, Secondary and tertiary structures of gaseous protein ions characterized by electron capture dissociation mass spectrometry and photofragment spectroscopy, Proc. Natl. Acad. Sci. U.S.A. 99 (2002) 15863-15868.

[47] D. Oepts, A.F.G. van der Meer, P.W. van Amersfoort, The Free-Electron-Laser User Facitilty FELIX, Infrared Phys. Technol. 36 (1995) 297-308.

[48] T. Marino, N. Russo, M. Toscano, Interaction of Li^+, Na^+, and K^+ with the Proline Amino Acid. Complexation Modes, Potential Energy Profiles, and Metal Ion Affinities, J. Phys. Chem. B 107 (2003) 2588-2594.

[49] K.M. Lee, S.W. Park, I.S. Jeon, B.R. Lee, D.S. Ahn, S. Lee, Computational Study of Proline - Water Cluster, Bull. Korean Chem. Soc. 26 (2005) 909-912.

[50] A. Lesarri, S. Mata, E.J. Cocinero, S. Blanco, J.C. Lopez, J.L. Alonso, The Structure of Neutral Proline, Angew. Chem. Int. Ed. 41 (2002) 4673-4676.

[51] S.G. Stepanian, I.D. Reva, E.D. Radchenko, L. Adamowicz, Conformers of Nonionized Proline. Matrix-Isolation Infrared and Post-Hartree-Fock ab Initio Study, J. Phys. Chem. A 105 (2001) 10664-10672.

[52] R.M. Moision, P.B. Armentrout, The Special Five-Membered Ring of Proline: An Experimental and Theoretical Investigation of Alkali Metal Cation Interactions with Proline and Its Four- and Six-Membered Ring Analogues, J. Phys. Chem. A 110, (2006) 3933-3946.

[53] A.S. Lemoff, M.F. Bush, E.R. Williams, Structures of Cationized Proline Analogues: Evidence for the Zwitterionic Form, J. Phys. Chem. 109 (2005) 1903-1910.

[54] C. Kapota, J. Lemaire, P. Maître, G. Ohanessian, Vibrational Signature of Charge Solvation vs Salt Bridge Isomers of Sodiated Amino Acids in the Gas Phase, J. Am. Chem. Soc. 126 (2004) 1836-1842.

[55] H.Wincel, Hydration Energies of Sodiated Amino Acids from Gas-Phase Equilibria Determinations, J. Phys. Chem. A 111 (2007) 5784-5791.

[56] M.K. Drayß, D. Blunk, J. Oomens, M. Schäfer, Infrared Multiple Photon Dissociation Spectroscopy of Potassiated Proline, J. Phys. Chem. A 112 (2008) 11972-11974.

[57] G.J. Fleming, P.R. McGill and H. Idriss, Gas phase interaction of L-proline with Be^{2+}, Mg^{2+} and Ca^{2+} ions: a computational study, J. Phys. Org. Chem. 20 (2007) 1032-1042.

[58] M.F. Bush, M.W. Forbes, R.A. Jockusch, J. Oomens, N.C. Polfer, R.J. Saykally, E.R. Williams, Infrared Spectroscopy of Cationized Lysine and *ε*-*N*-methyllysine in the Gas Phase: Effects of Alkali-Metal Ion Size and Proton Affinity on Zwitterion Stability, J. Phys. Chem. A 111 (2007) 7753-7760.

[59] M.F. Bush, J. Oomens, J. Saykally, E.R. Williams, Alkali Metal Ion Binding to Glutamine and Glutamine Derivatives Investigated by Infrared Action Spectroscopy and Theory, J. Phys. Chem. A 112 (2008) 8578-8584.

[60] T. Wyttenbach, M. Witt, M.T. Bowers, On the Stability of Amino Acid Zwitterions in the Gas Phase: The Influence of Derivatization, Proton Affinity, and Alkali Ion Addition, J. Am. Chem. Soc. 122 (2000) 3458-3464.

[61] T. Wyttenbach, M. Witt, M.T. Bowers, On the question of salt bridges of cationized amino acids in the gas phase: glycine and arginine, Int. J. Mass Spectrom. 182/183 (1999) 243-252.

[62] M.F. Bush, J. Oomens, E.R. Williams Proton Affinity and Zwitterion Stability: New Results from Infrared Spectroscopy and Theory of Cationized Lysine and Analogues in the Gas Phase, J. Phys. Chem. A 113 (2009) 431-438.

[63] L. Aurelio, J.S. Box, R.T.C. Brownlee, A.B. Huges, M.M. Sleebs, An Efficient Synthesis of *N*-Methyl Amino Acids by Way of Intermediate 5-Oxazolidinones, J. Org. Chem. 68 (2003) 2652-2667.

[64] R.L. Elliott, H. Kopecka, N.-H. Lin, Y. He, D.S. Garvey, A Short, Efficient Synthesis of the Novel Cholinergic Channel Activator, ABT 418, from L-Proline, Synthesis (1995) 772-774.

[65] N. Polfer, J. Oomens, Reaction products in mass spectrometry elucidated with infrared spectroscopy, Phys. Chem. Chem. Phys. 9 (2007) 3804-3817.

[66] J.J. Valle, J.R. Eyler, J. Oomens, D.T. Moore, A.F.G. van der Meer, G. von Helden, G. Meijer, C.L. Hendrickson, A.G. Marshall, G.T. Blakney, Free electron laser-Fourier transform ion cyclotron resonance mass spectrometry facility for obtaining infrared multiphoton dissociation spectra of gaseous ions, Rev. Sci. Instrum. 76 (2005) 023103.

[67] N.C. Polfer, J. Oomens, D.T. Moore, G. von Helden, G. Meijer, R.C. Dunbar, Infrared Spectroscopy of Phenylalanine Ag(I) and Zn(II) Complexes in the Gas Phase, J. Am. Chem. Soc. 128 (2006) 517-525.

[68] M.J. Frisch, G.W. Trucks, H.B. Schlegel, G.E. Scuseria, M.A. Robb, J.R. Cheeseman, J.A., Jr. Montgomery, T. Vreven, K.N. Kudin, J.C. Burant, J.M. Millam, S.S. Iyengar, J. Tomasi, V. Barone, B. Mennucci, M. Cossi, G. Scalmani, N. Rega, G.A. Petersson, H. Nakatsuji, M. Hada, M. Ehara, K. Toyota, R. Fukuda, J. Hasegawa, M. Ishida, T. Nakajima, Y. Honda, O. Kitao, H. Nakai, M. Klene, X. Li, J.E. Knox, H.P. Hratchian, J.B. Cross, V. Bakken, C. Adamo, J. Jaramillo, R. Gomperts, R.E. Stratmann, O. Yazyev, A.J. Austin, R. Cammi, C. Pomelli, J.W. Ochterski, P.Y. Ayala, K. Morokuma, G.A. Voth, P. Salvador, J.J. Dannenberg, V.G. Zakrzewski, S. Dapprich, A.D. Daniels, M.C. Strain, O. Farkas, D.K. Malick, A.D. Rabuck, K. Raghavachari, J.B. Foresman, J.V. Ortiz, Q. Cui, A.G. Baboul, S. Clifford, J. Cioslowski, B.B. Stefanov, G. Liu, A. Liashenko, P. Piskorz, I. Komaromi, R.L. Martin, D.J. Fox, T. Keith, M.A. Al-Laham, C.Y. Peng, A. Nanayakkara, M. Challacombe, P.M.W. Gill, B. Johnson, W. Chen, M.W.Wong, C. Gonzalez, J.A. Pople, *Gaussian 03*, revision D.01; Gaussian, Inc.: Wallingford, CT, 2004.

[69] T. Leininger, A. Nicklass, W. Kiichle, H. Stoll, M. Dolg, A. Bergner, The accuracy of the pseudopotential approximation: non-frozen-core effects for spectroscopic constants of alkali fluorides XF (X = K, Rb, Cs), Chem. Phys. Lett. 255 (1996) 274-280.

[70] K.L. Schuchardt, B.T. Didier, T. Elsethagen, L. Sun, V. Gurumoorthi, J. Chase, J. Li, T.L. Windus, Basis Set Exchange: A Community Database for Computational Sciences, J. Chem. Inf. Model., 47 (2007) 1045-1052.

[71] N. Polfer, J. Oomens, R.C. Dunbar, IRMPD spectroscopy of metal/tryptophan complexes, Phys. Chem. Chem. Phys. 8 (2006) 2744-2751.

[72] http://www.chemcraftprog.com

[73] R.M. Moision, P.B. Armentrout, An Experimental and Theoretical Dissection of Sodium Cation/Glycine Interactions, J. Phys. Chem. A 106 (2002) 10350-10362.

[74] R.M. Moision, P.B. Armentrout, An Experimental and Theoretical Dissection of Potassium Cation/Glycine Interactions, Phys. Chem. Chem. Phys. 6 (2004) 2588-2599.

[75] R. Wu, T.B. McMahon, Infrared Multiple Photon Dissociation Spectra of Proline and Glycine Proton-Bound Homodimers. Evidence for Zwitterionic Structure, J. Am. Chem. Soc. 129 (2007) 4864-4865.

[76] N. Polfer, B. Paizs, L.C. Snoek, I. Compagnon, S. Suhai, G. Meijer, G. von Helden, J. Oomens, Infrared Fingerprint Spectroscopy and Theoretical Studies of Potassium Ion Tagged Amino Acids and Peptides in the Gas Phase, J. Am. Chem. Soc. 127 (2005) 8571-8579.

[77] G.N. Patwari, J.M. Lisy, Cyclohexane as a Li^+ Selective Ionophore, J. Phys. Chem. A 111 (2007) 7585-7588.

[78] R.G. Pearson, J. Songstad, Application of the Principle of Hard and Soft Acids and Bases to Organic Chemistry, J. Am. Chem. Soc. 89 (1967) 1827-1836.

[79] R.G. Pearson (ed.) Hard and Soft Acids and Bases, Dowden & Hutchinson & Ross Inc., Stroudsburg, PA, 1973.

[80] M.T. Rodgers, P.B. Armentrout, A Critical Evaluation of the Experimental and Theoretical Determination of Lithium Cation Affinities, Int. J. Mass Spectrom. 267 (2007) 167-182.

Figure captions

Figure 1. IRMPD spectra of alkali metal cationized molecular ions of proline (M^+Pro) with $M^+ = Li^+, Na^+, K^+, Rb^+$, and Cs^+.

Figure 2. Lowest energy gas-phase ion structures of K^+Pro, computed at the B3LYP/6-311++G(2d,2p) level of theory. Relative energies of the respective conformers are listed in Table 1.

Figure 3. IRMPD spectra of K^+Pro,[56] K^+*N*-methyl proline,[24] and K^+*N*-methyl-proline-methylester.

Figure 4. IRMPD spectrum of potassiated *N*-methyl proline compared to the computed absorptions of the most stable SB[CO_2^-]C3d structure of K^+*N*-methyl proline identified by theory.[24]

Figure 5. IRMPD spectrum of Li^+Pro and calculated spectra of the two most stable SB and CS conformers. All conformers of Li^+Pro computed at the B3LYP/6-311++G(2d,2p) level of theory are presented in Figure 1S in the supporting information.

Figure 6. IRMPD spectrum of Cs^+Pro and calculated spectra of the two most stable SB and CS conformers. Additional conformers of Cs^+Pro identified by theory are presented in Figure 9S and 10S in the supporting information

Figure 7. Difference of the relative energies ($\Delta\Delta H_0$) of the most stable SB and CS conformer of alkali metal cationized amino acids [amino acid + M]$^+$ in kJ mol^{-1} versus respective alkali metal cation ($M^+ = Li^+, Na^+, K^+, Rb^+$, and Cs^+). The alkali metal cations are ordered according to increasing ion size. The data sets of the amino acids Arg, Trp, Ser, Asp and Met were taken from references 33, 70, 29, 31, and 32, respectively. Relative energies of all conformers identified by theory of alkali metalized *N*-methyl glycine and glycine are listed in Tables 1S and 2S, respectively, in the supporting information.

Figure 8. IRMPD-spectra of alkali metal cationized molecular ions of *N*-methyl alanine (M^+*N*-methyl alanine) with $M^+ = Li^+$, Na^+, K^+, Rb^+, and Cs^+.

Figure 9. IRMPD spectrum of Na^+*N*-methyl alanine and calculated spectra of the two most stable SB and CS conformers. All conformers of Na^+*N*-methyl alanine identified by theory are presented in Figure 15S in the supporting information.

Figure 10. IRMPD spectrum of Cs^+*N*-methyl alanine and calculated spectra of the two most stable SB and CS conformers. All conformers of Cs^+*N*-methyl alanine identified by theory are presented in Figure 20S in the supporting information.

Figure 1

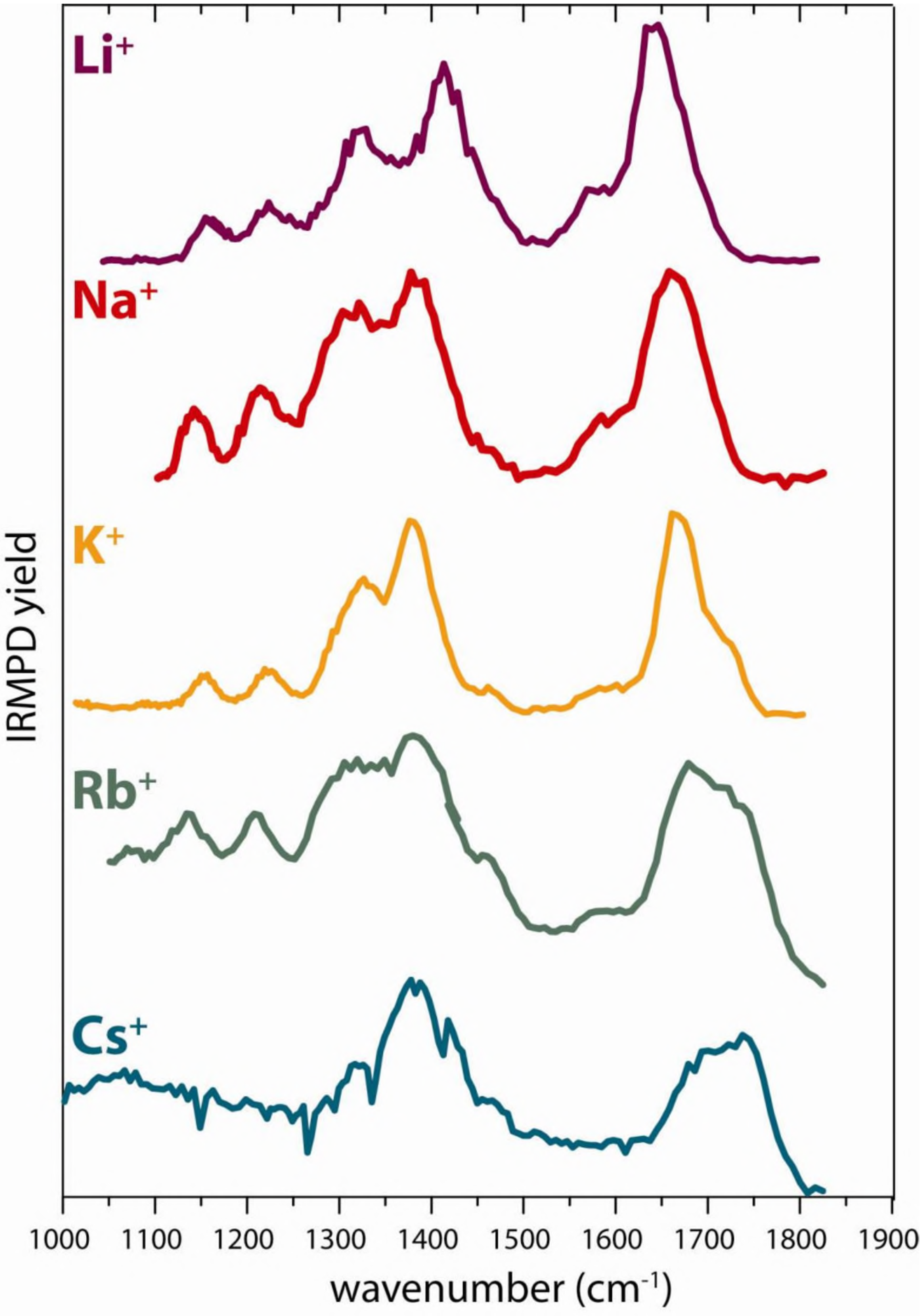
Li+
Na+
K+
Rb+
Cs+
IRMPD yield
1000
1100
1200
1300
1400
1500
1600
1700
1800
1900
wavenumber (cm-1)

Figure 2

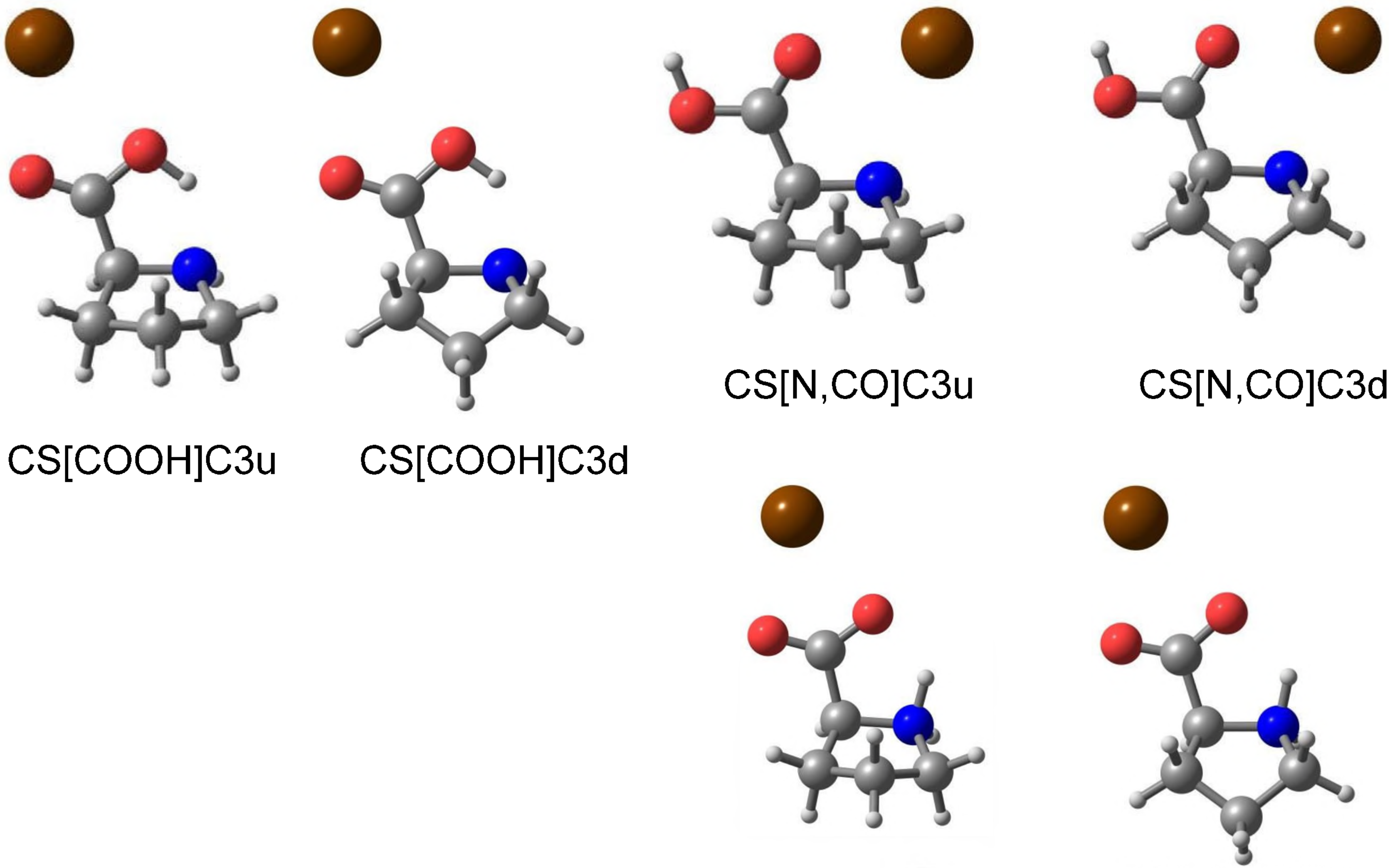

CS[COOH]C3u CS[COOH]C3d

CS[N,CO]C3u CS[N,CO]C3d

SB[CO_2^-]C3u SB[CO_2^-]C3d

Figure 3

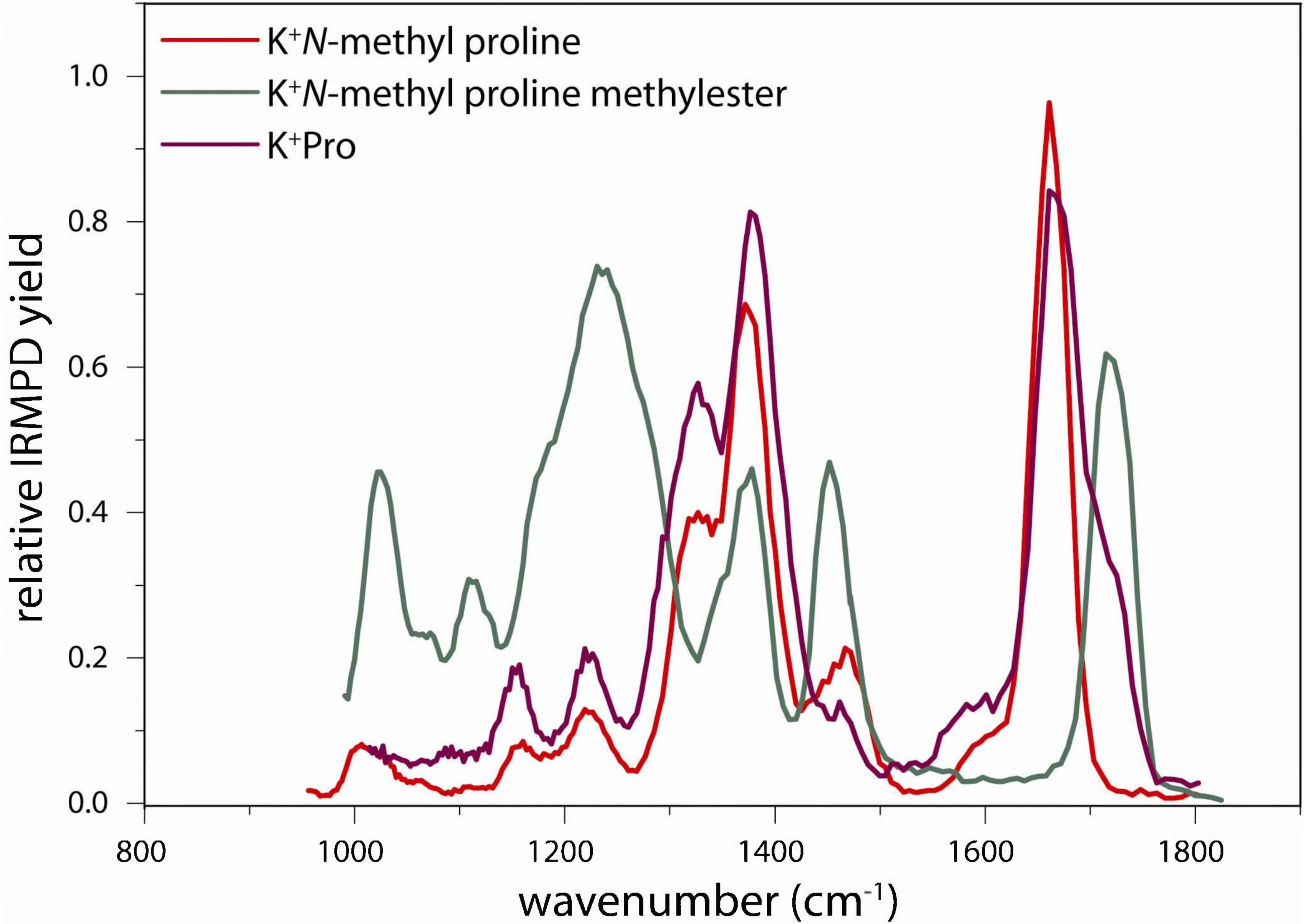

K+N-methyl proline
K+N-methyl proline methylester
K+Pro
relative IRMPD yield
0.0
0.2
0.4
0.6
0.8
1.0
wavenumber (cm-1)
800
1000
1200
1400
1600
1800

Figure 4

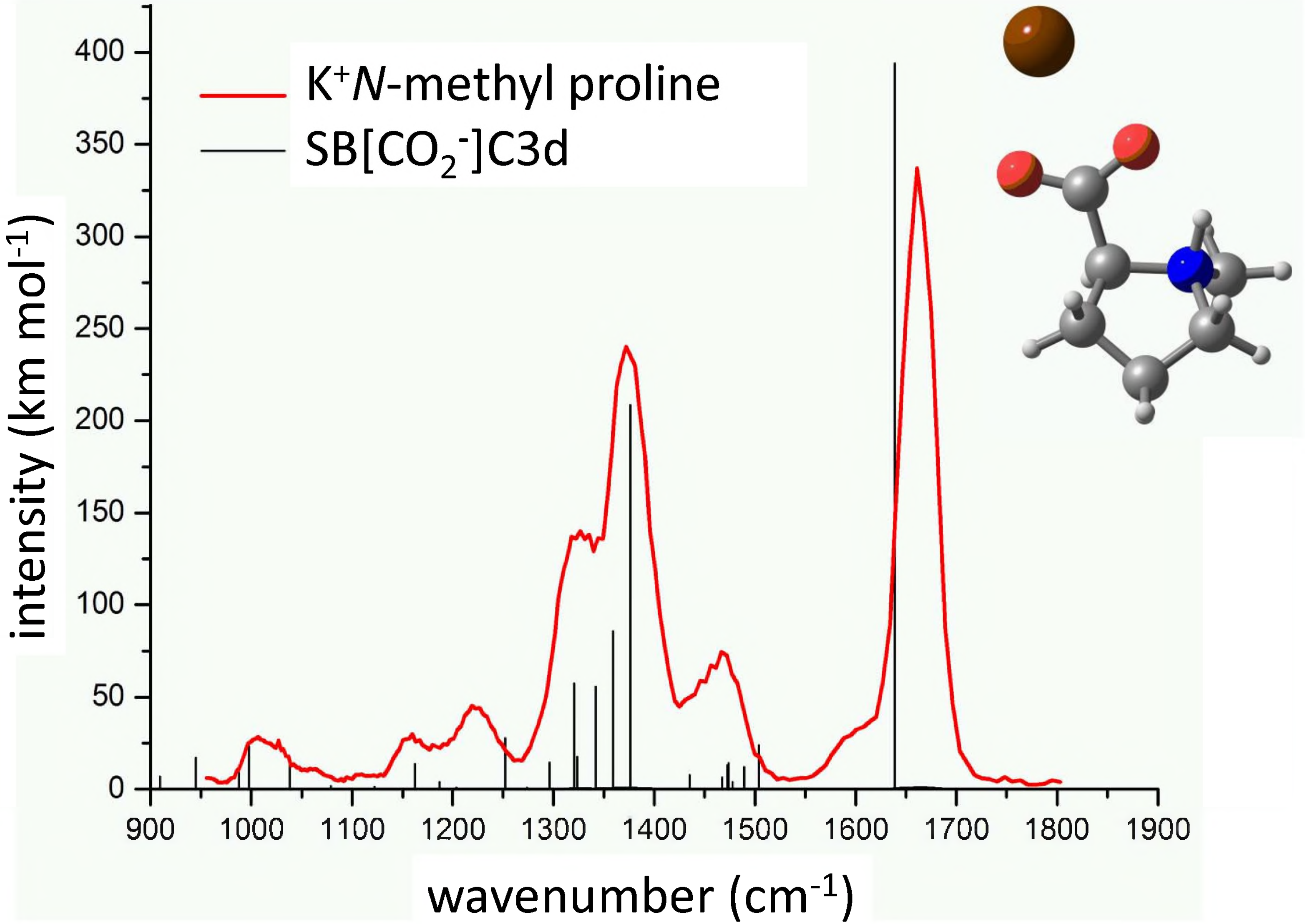

K+N-methyl proline
SB[CO2-]C3d
intensity (km mol-1)
400
350
300
250
200
150
100
50
0
900
1000
1100
1200
1300
1400
1500
1600
1700
1800
1900
wavenumber (cm-1)

Figure 5

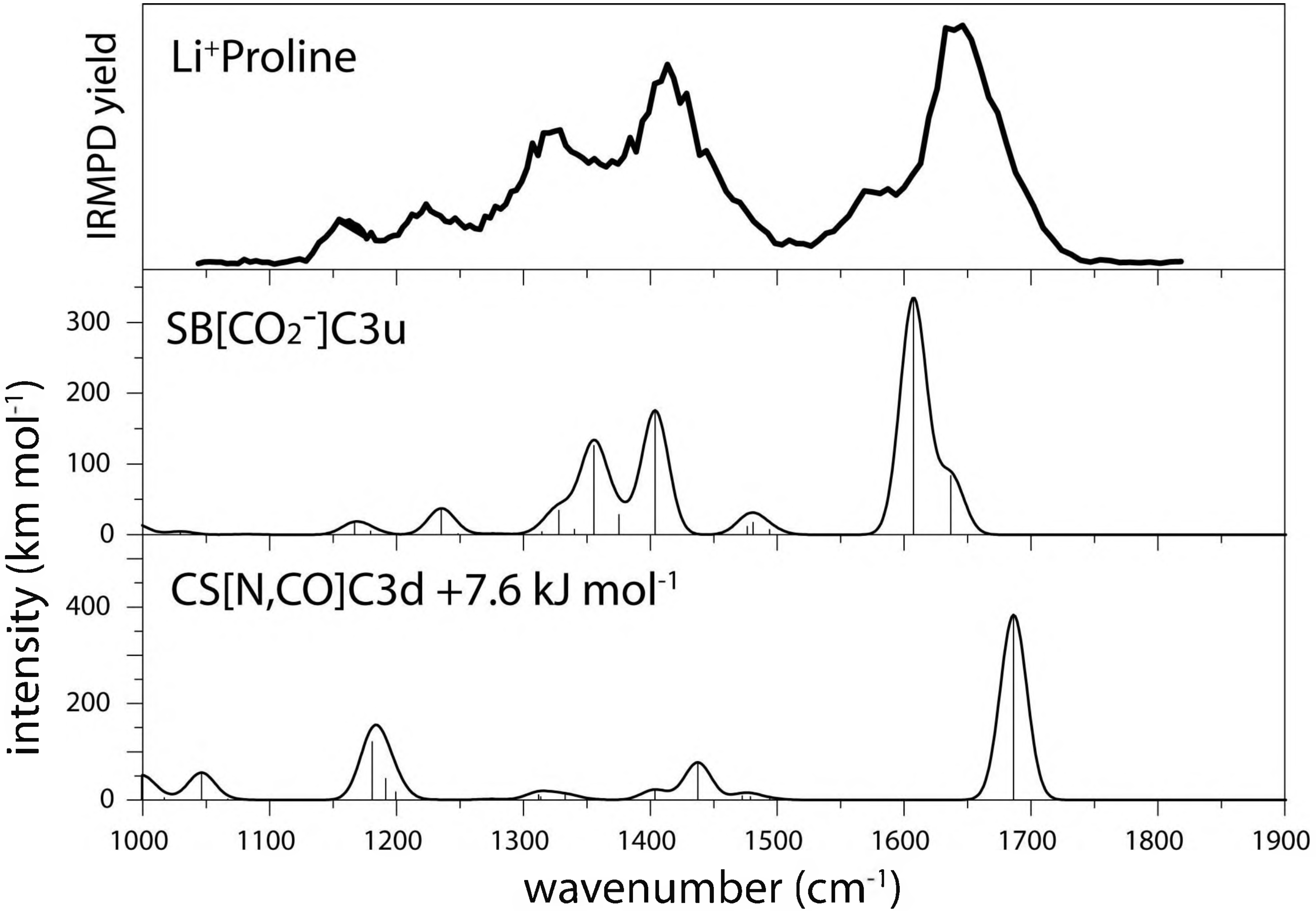
Li⁺Proline
IRMPD yield
SB[CO₂⁻]C3u
300
200
100
0
CS[N,CO]C3d +7.6 kJ mol⁻¹
400
200
0
intensity (km mol⁻¹)
1000
1100
1200
1300
1400
1500
1600
1700
1800
1900
wavenumber (cm⁻¹)

Figure 6

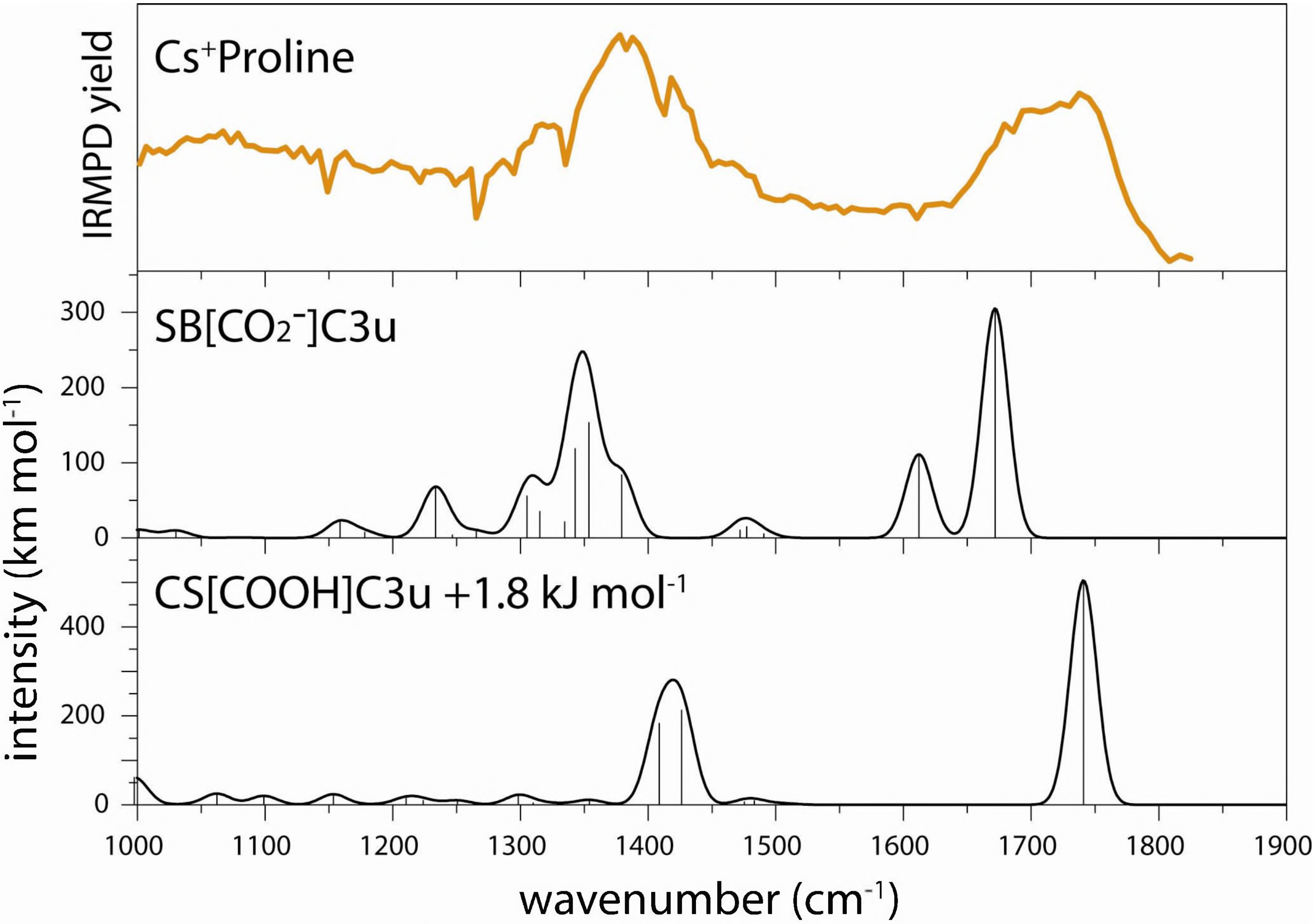

IRMPD yield
Cs⁺Proline
SB[CO2⁻]C3u
CS[COOH]C3u +1.8 kJ mol⁻¹
intensity (km mol⁻¹)
0
100
200
300
0
200
400
1000
1100
1200
1300
1400
1500
1600
1700
1800
1900
wavenumber (cm⁻¹)

Figure 7

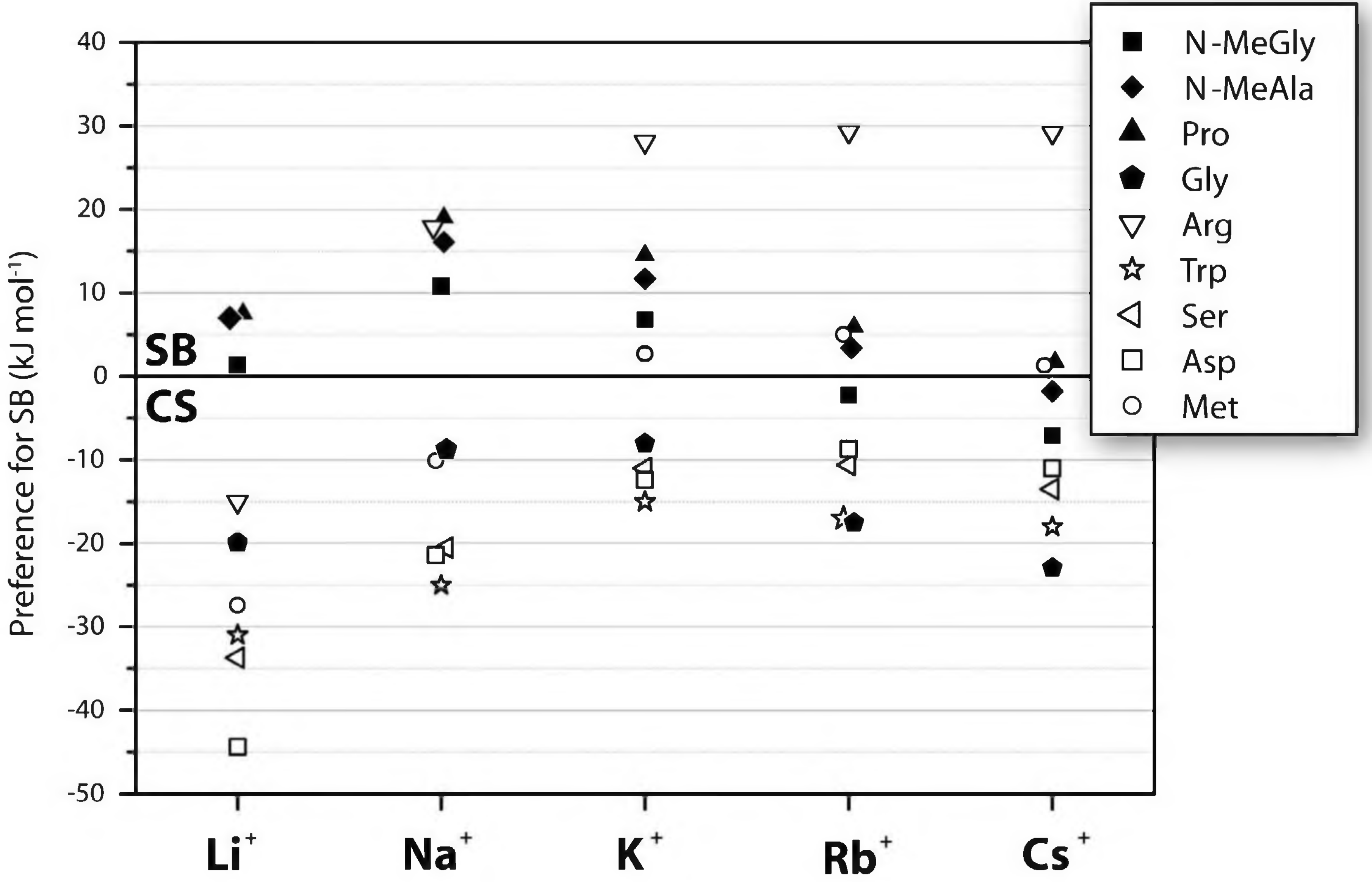
Preference for SB (kJ mol-1)
40
30
20
10
0
-10
-20
-30
-40
-50
SB
CS
Li+
Na+
K+
Rb+
Cs+
■ N-MeGly
◆ N-MeAla
▲ Pro
⬟ Gly
▽ Arg
☆ Trp
◁ Ser
□ Asp
○ Met

Figure 8

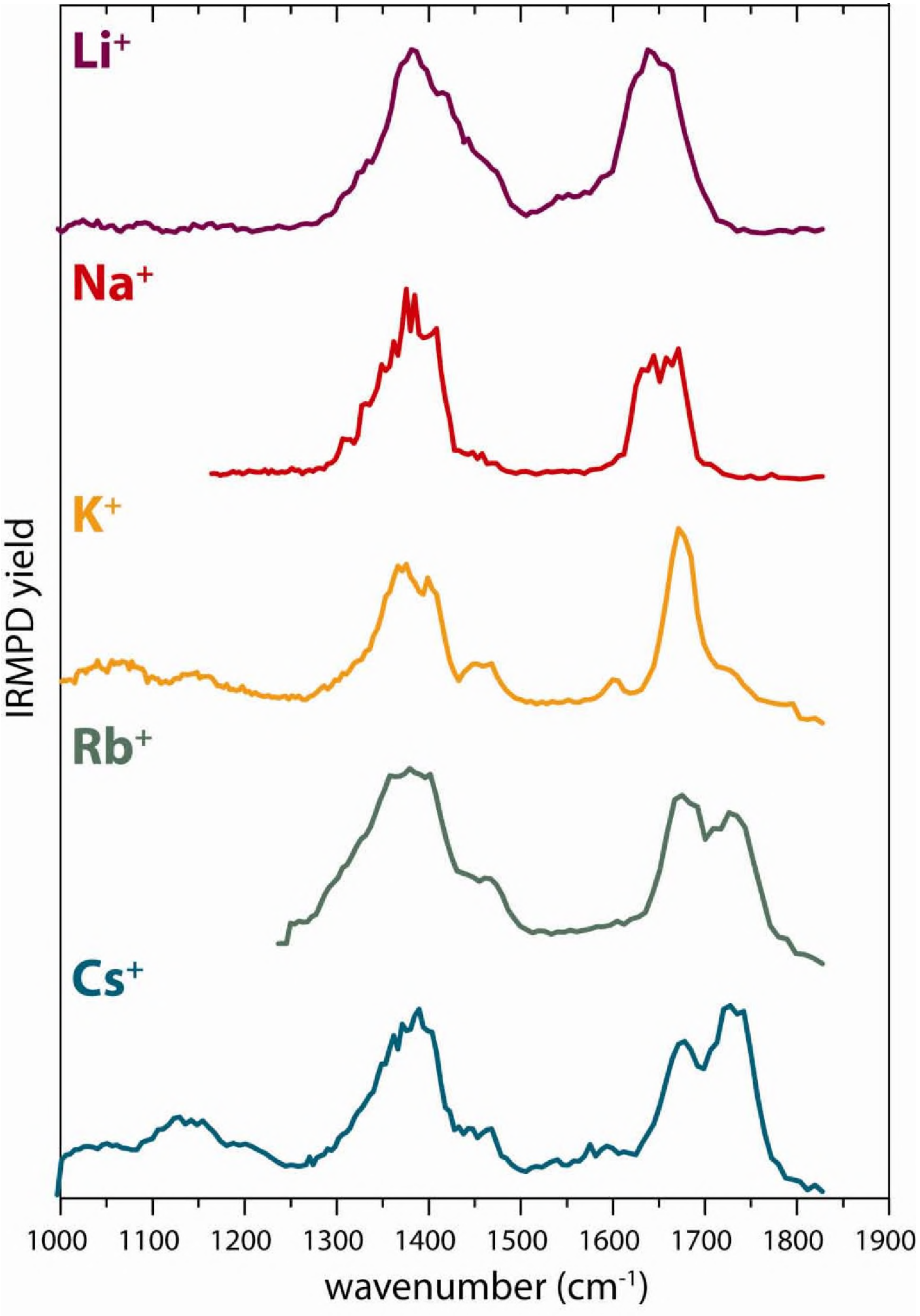
Li⁺
Na⁺
K⁺
Rb⁺
Cs⁺
IRMPD yield
1000
1100
1200
1300
1400
1500
1600
1700
1800
1900
wavenumber (cm⁻¹)

Figure 9

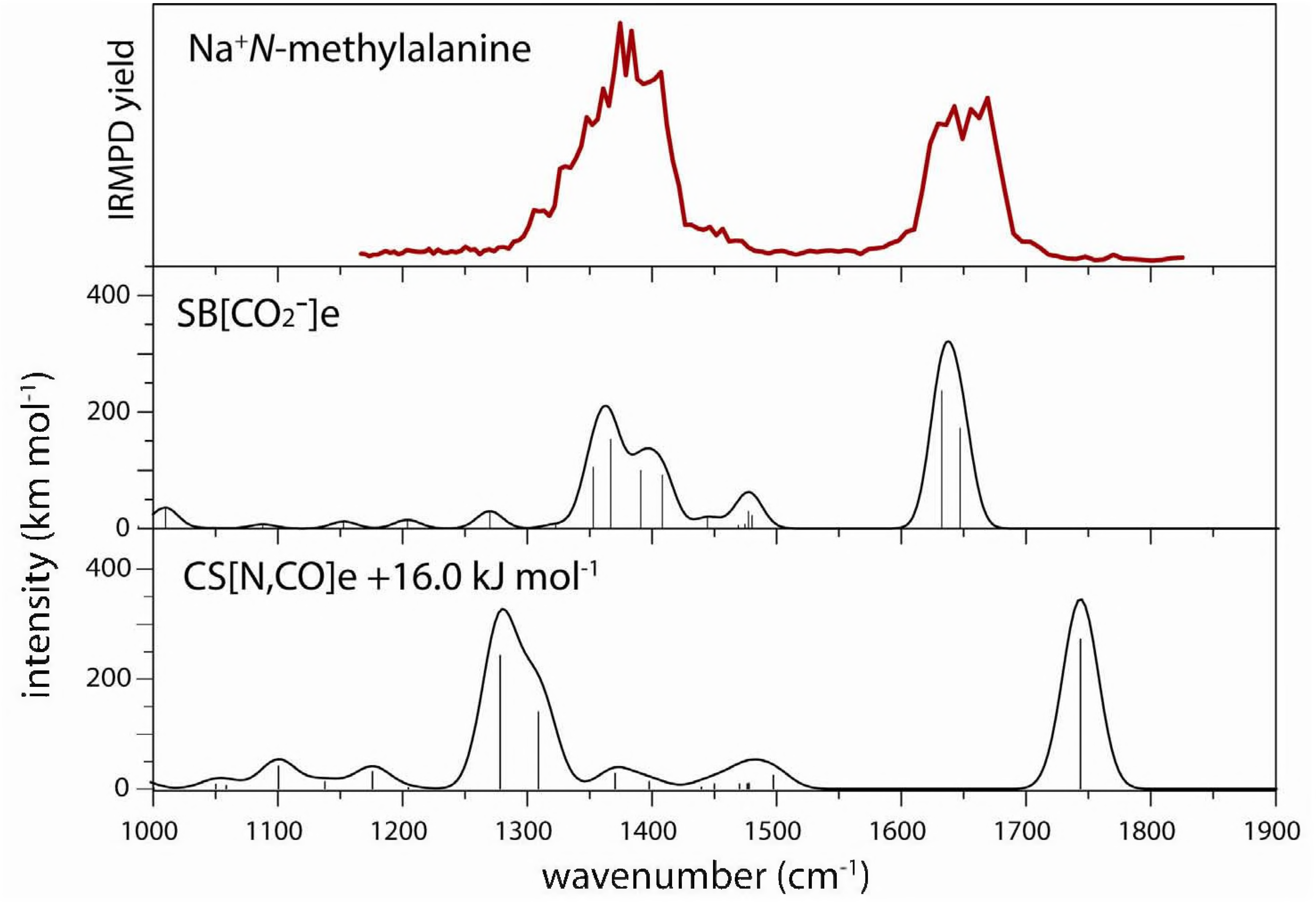
IRMPD yield
Na$^+$*N*-methylalanine
SB[CO$_2^-$]e
CS[N,CO]e +16.0 kJ mol^{-1}
intensity (km mol^{-1})
400
200
0
400
200
0
1000
1100
1200
1300
1400
1500
1600
1700
1800
1900
wavenumber (cm^{-1})

Figure 10

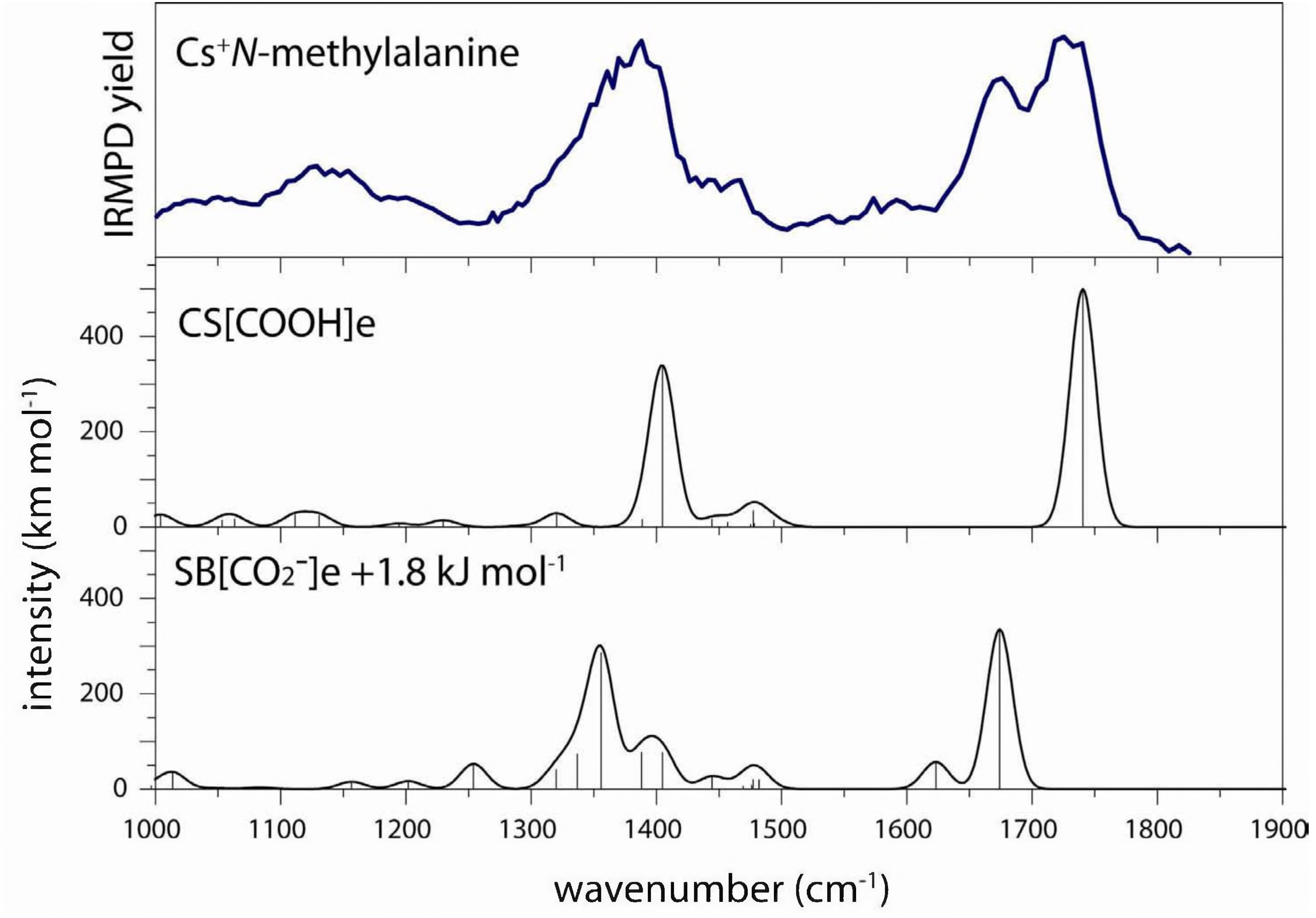
Cs$^+$*N*-methylalanine
IRMPD yield
CS[COOH]e
SB[CO$_2^-$]e +1.8 kJ mol^{-1}
intensity (km mol^{-1})
0
200
400
0
200
400
1000
1100
1200
1300
1400
1500
1600
1700
1800
1900
wavenumber (cm^{-1})

Supplementary Material

IR Spectroscopy of cationized aliphatic amino acids: Stability of charge-solvated structure increases with metal cation size

Miriam K. Drayß, Peter B. Armentrout, Jos Oomens* and
Mathias Schäfer*

International Journal of Mass Spectrometry 2010

Figure 1S. Lowest energy gas-phase ion structures of Li$^+$Pro, computed at the B3LYP/6-311++G(2d,2p) level of theory. Relative energies of the respective isomers are listed in Table 1.

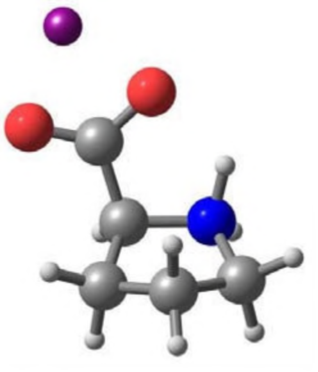

SB[CO$_2^-$]C3u

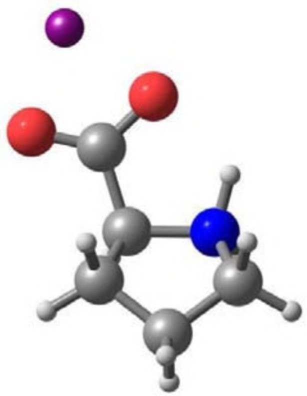

SB[CO$_2^-$]C3d

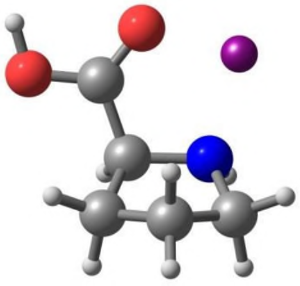

CS[N,CO]C3u

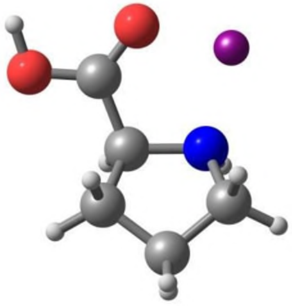

CS[N,CO]C3d

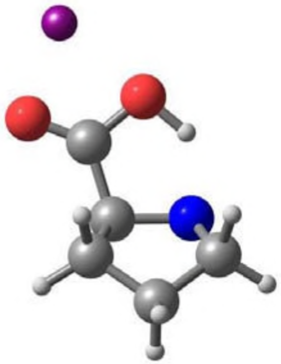

CS[COOH]C3d

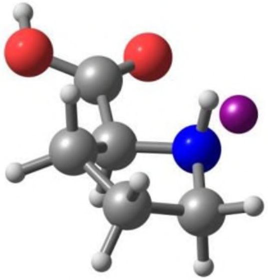

CS[N,CO]NHu

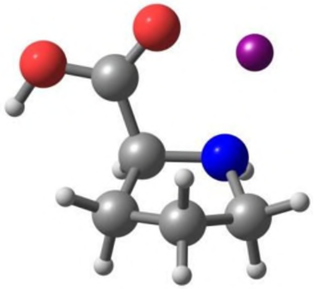

CS[N,CO]C3u,tOH

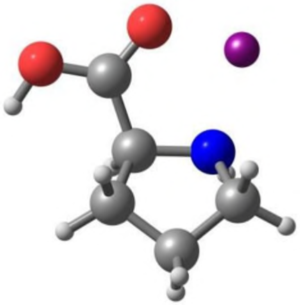

CS[N,CO]C3d,tOH

Figure 2S. IRMPD spectrum of Na$^+$Pro and calculated spectra of the two most stable isomers SB[CO$_2^-$]C3u and CS[N,CO]C3u computed at the B3LYP/6-311++G(2d,2p) level of theory. The moderate IRMPD detection efficiency of this experiment is related to the high ICR frequency of the product ion Na$^+$ (*m/z* 23).

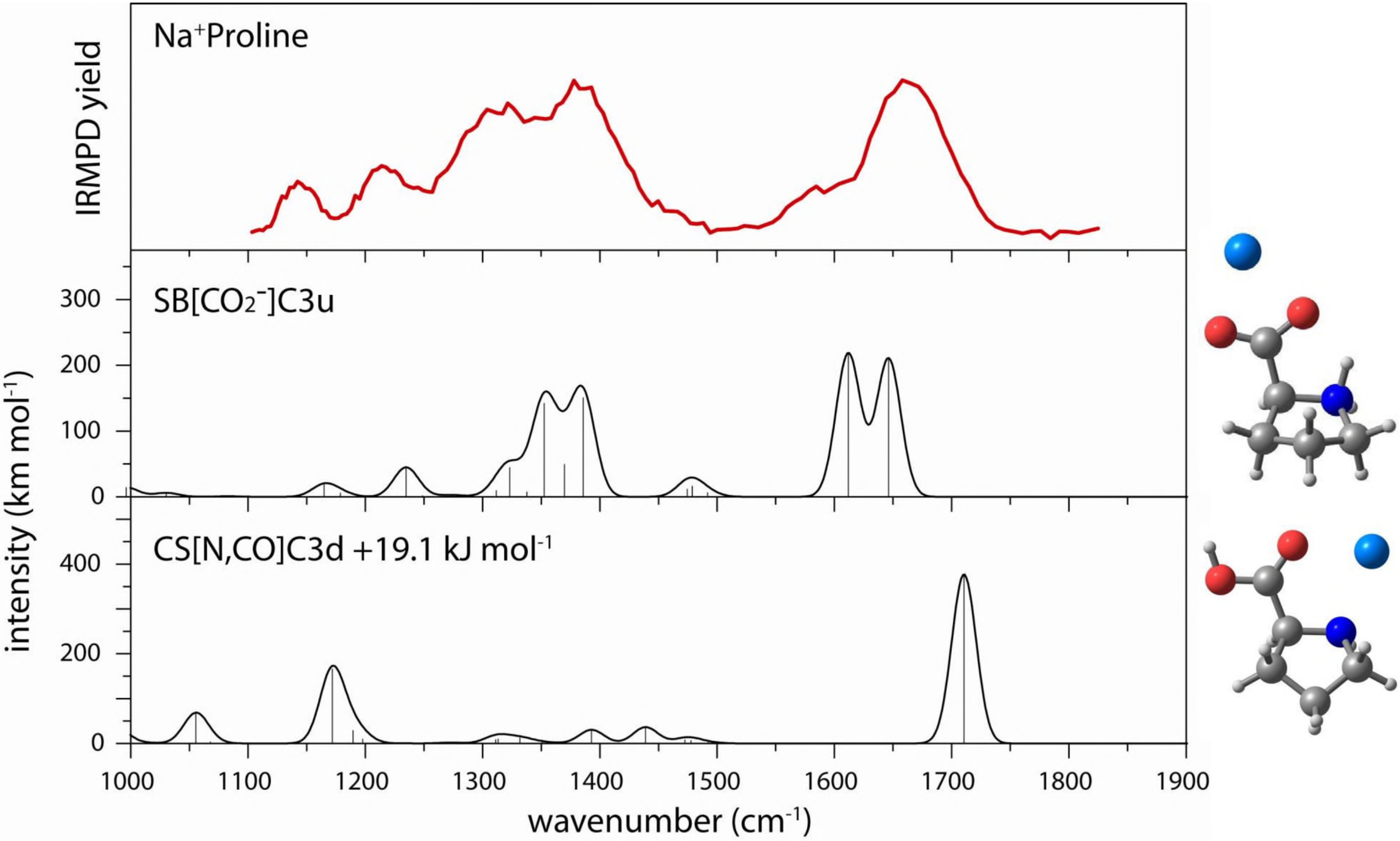

Figure 3S. Lowest energy gas-phase ion structures of Na$^+$Pro, computed at the B3LYP/6-311++G(2d,2p) level of theory. Relative energies of the respective isomers are listed in Table 1.

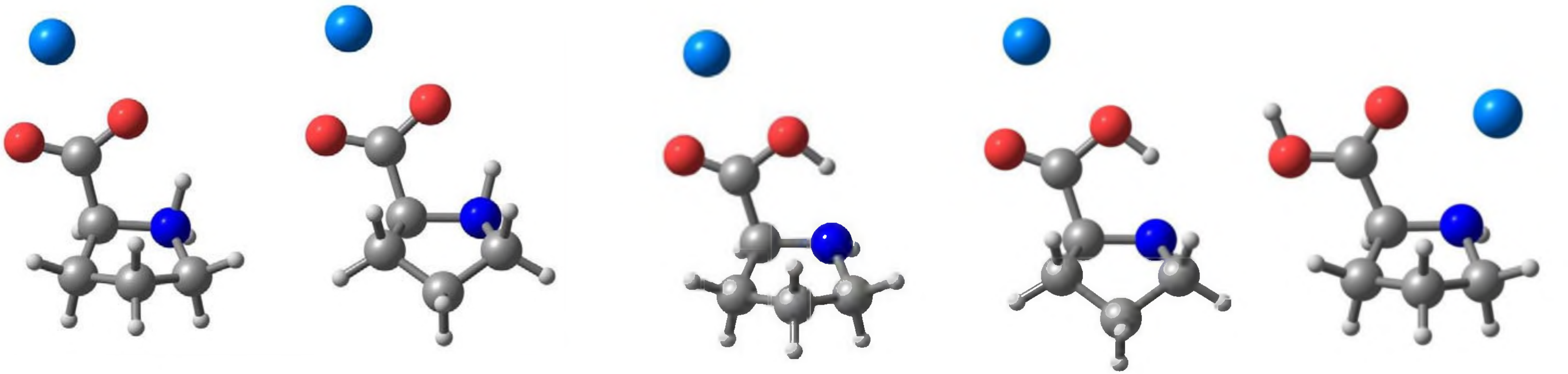

SB[CO$_2^-$]C3u SB[CO$_2^-$]C3d CS[COOH]C3u CS[COOH]C3d CS[N,CO]C3u

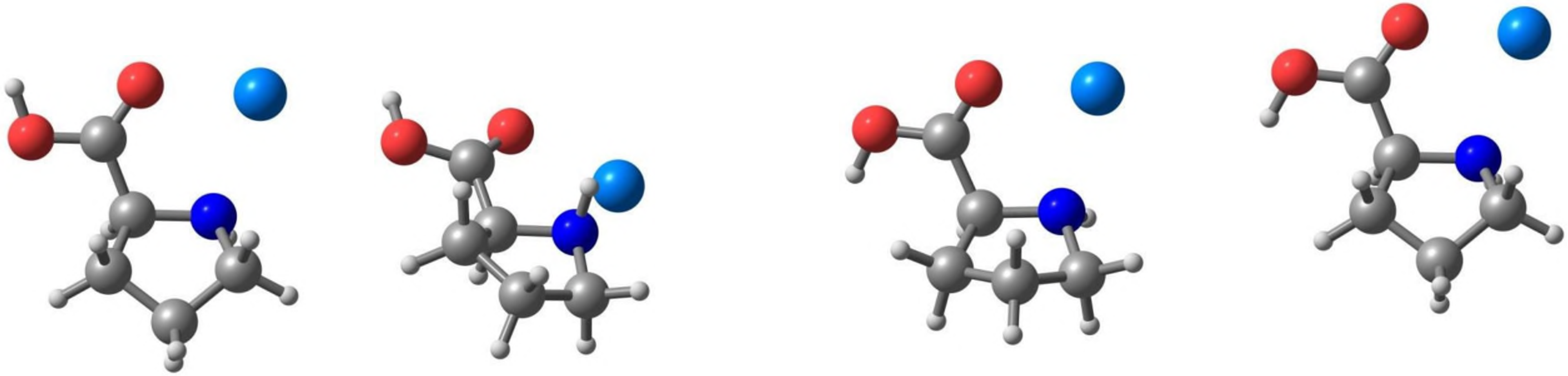

CS[N,CO]C3d CS[N,CO]NHu CS[N,CO]C3u,tOH CS[N,CO]C3d,tOH

Figure 4S. IRMPD spectrum of K^+Pro and calculated spectra of the two most stable isomers SB[CO_2^-]C3u and CS[COOH]C3u computed at the B3LYP/6-311++G(2d,2p) level of theory.

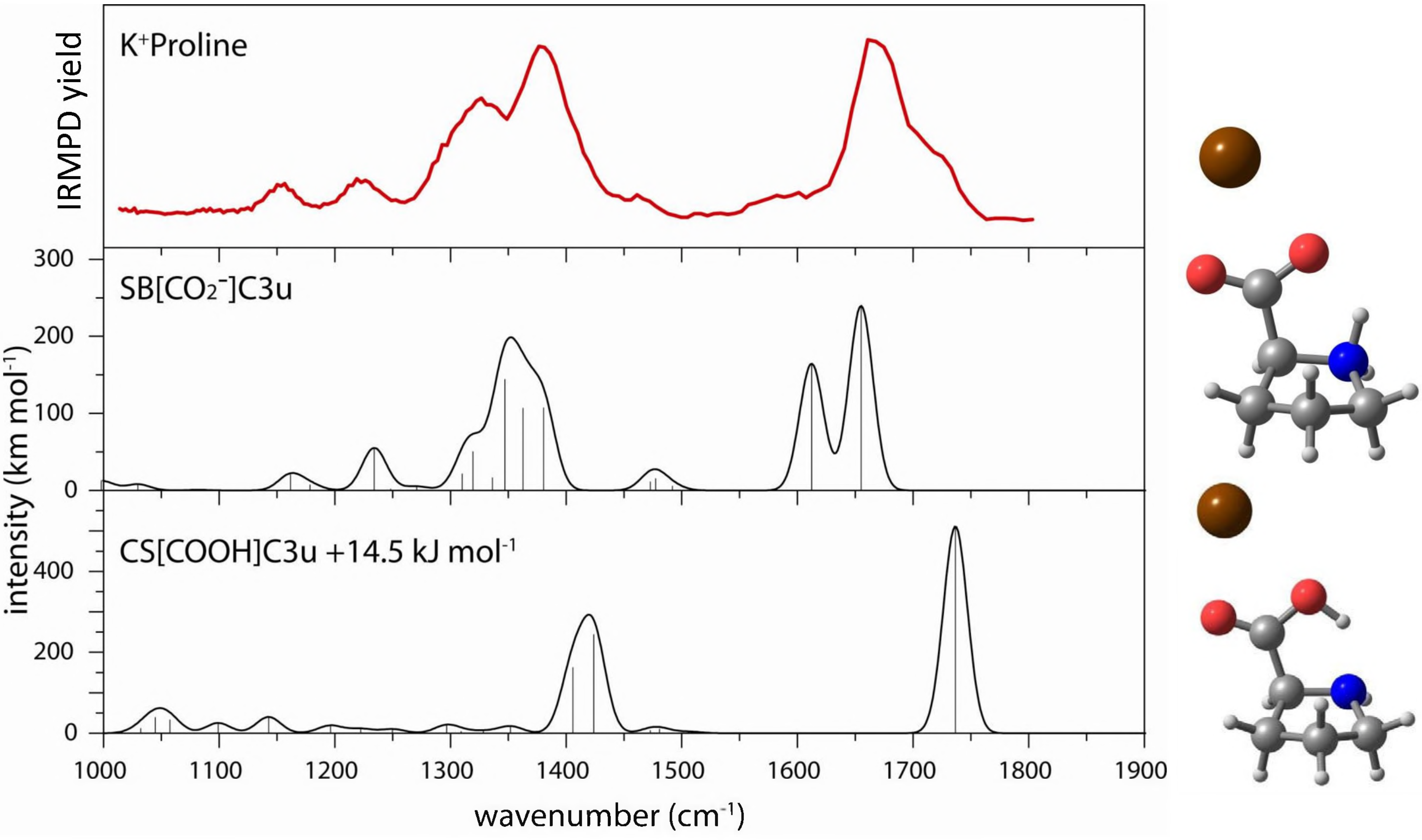

Figure 5S. Additional gas-phase ion structures of K$^+$Pro, computed at the B3LYP/6-311++G(2d,2p) level of theory. Relative energies of the respective isomers are listed in Table 1.

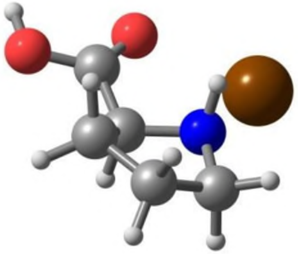

CS[N,CO]NHu

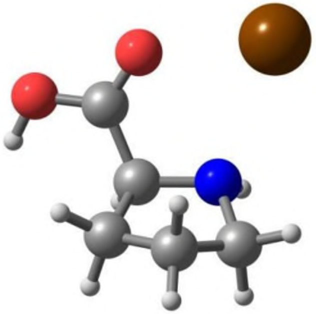

CS[N,CO]C3u,tOH

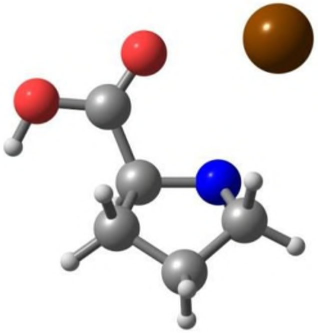

CS[N,CO]C3d,tOH

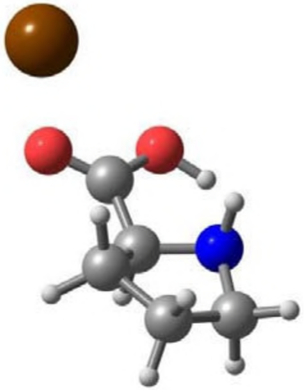

CS[COOH]NHu

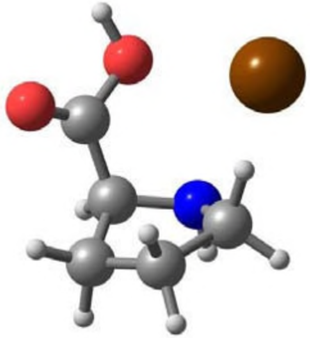

CS[N,OH]C3u

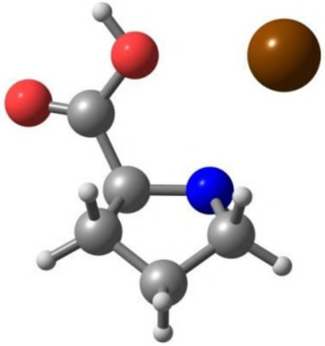

CS[N,OH]C3d

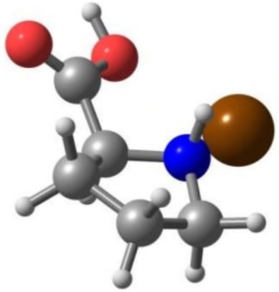

CS[N,OH]NHu

Figure 6S. IRMPD spectrum of Rb$^+$Pro and calculated spectra of the two most stable isomers SB[CO$_2^-$]C3u and CS[COOH]C3u computed at the B3LYP/6-311++G(2d,2p) level of theory.

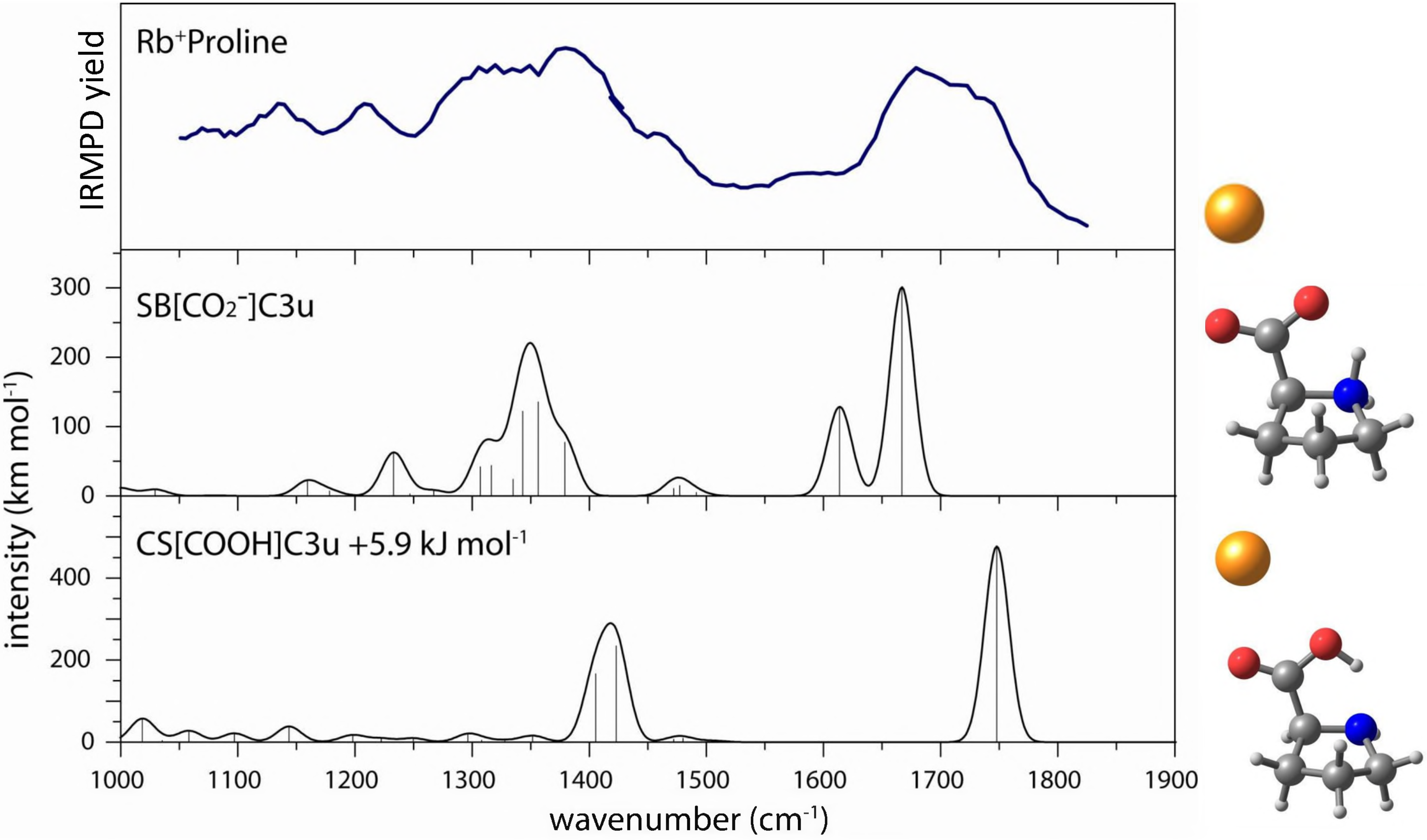

Figure 7S. Lowest energy gas-phase ion structures of Rb^+Pro, computed at the B3LYP/6-311++G(2d,2p) level of theory. Relative energies of the respective isomers are listed in Table 1.

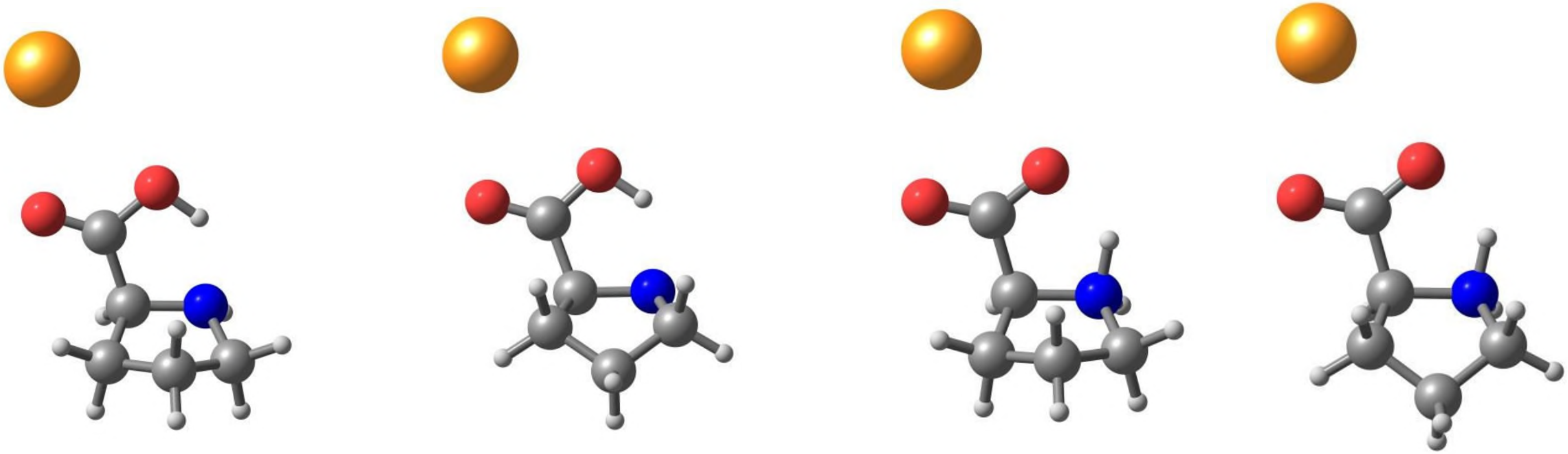

CS[COOH]C3u CS[COOH]C3d SB[CO$_2^-$]C3u SB[CO$_2^-$]C3d

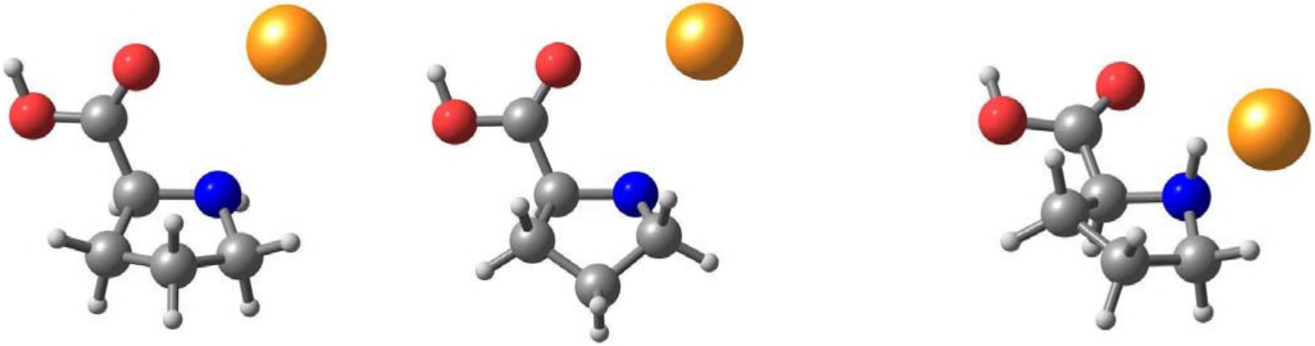

CS[N,CO]C3u CS[N,CO]C3d CS[N,CO]NHu

Figure 8S. Lowest energy gas-phase ion structures of Rb^+Pro, computed at the B3LYP/6-311++G(2d,2p) level of theory. Relative energies of the respective isomers are listed in Table 1.

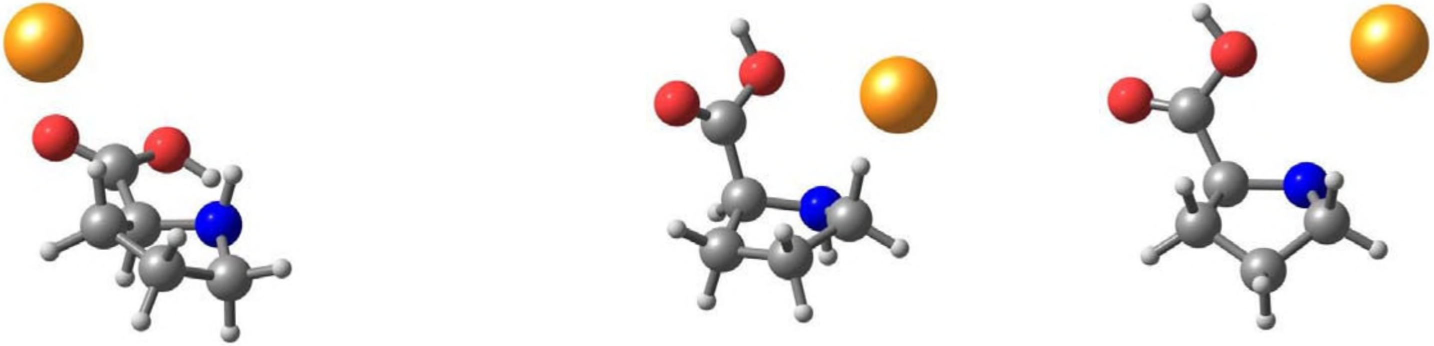

CS[COOH]NHu CS[N,OH]C3u CS[N,OH]C3d

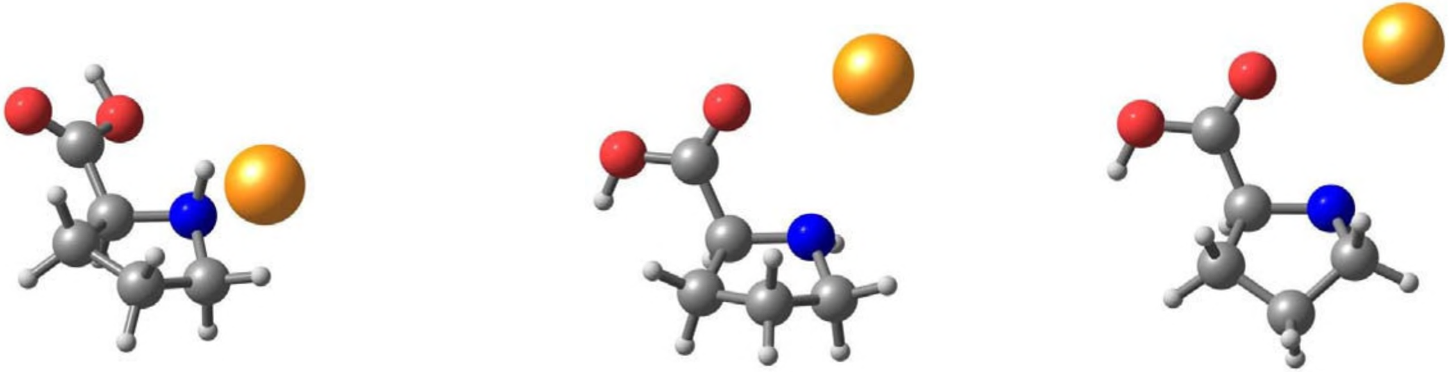

CS[N,OH]NHu CS[N,CO]C3u,tOH CS[N,CO]C3d,tOH

Figure 9S. Lowest energy gas-phase ion structures of Cs$^+$Pro, computed at the B3LYP/6-311++G(2d,2p) level of theory. Relative energies of the respective isomers are listed in Table 1.

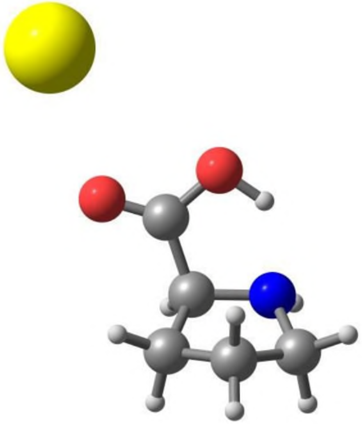

CS[COOH]C3u

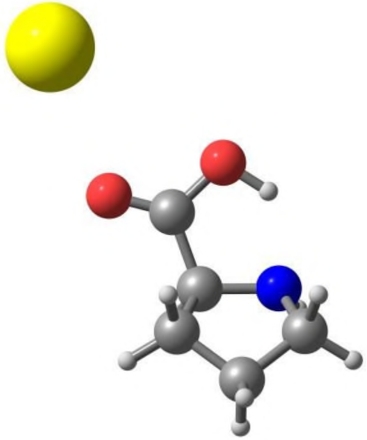

CS[COOH]C3d

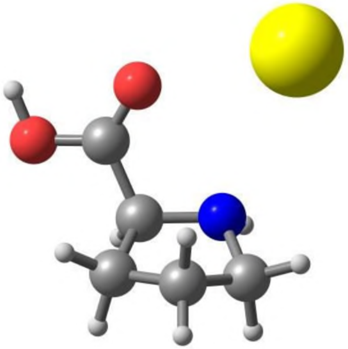

CS[N,CO]C3u

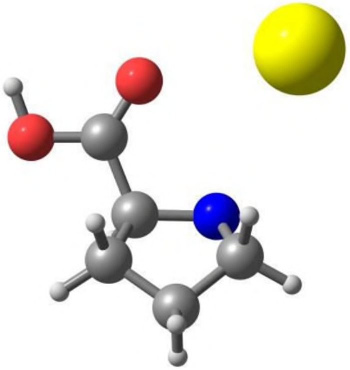

CS[N,CO]C3d

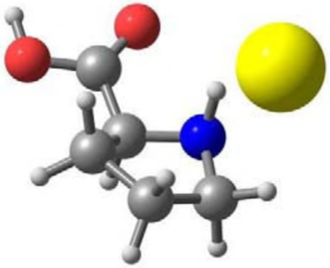

CS[N,CO]NHu

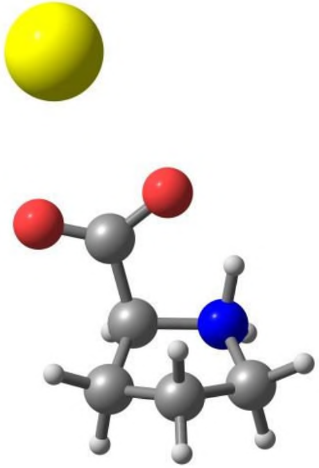

SB[CO$_2^-$]C3u

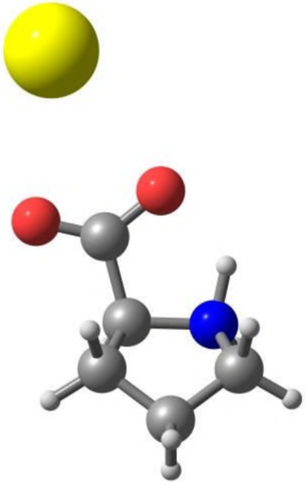

SB[CO$_2^-$]C3d

Figure 10S. Lowest energy gas-phase ion structures of Cs^+Pro, computed at the B3LYP/6-311++G(2d,2p) level of theory. Relative energies of the respective isomers are listed in Table 1.

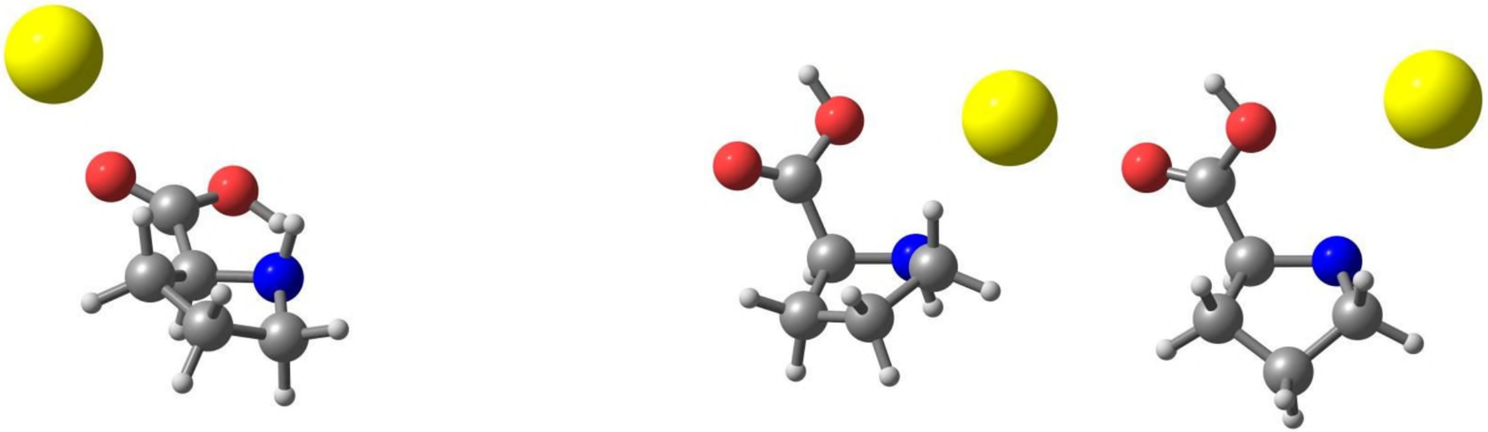

CS[COOH]NHu

CS[N,OH]C3u

CS[N,OH]C3d

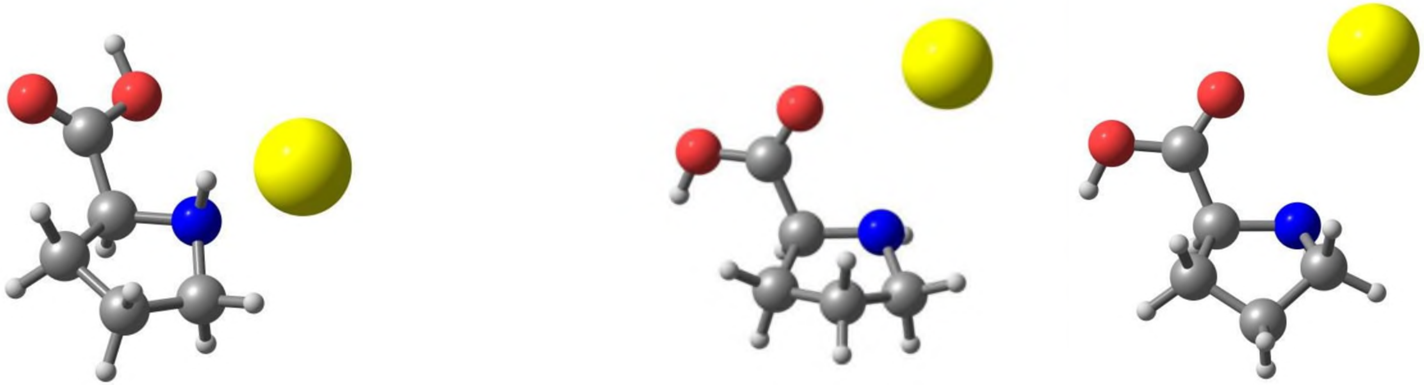

CS[N,OH]NHu

CS[N,CO]C3u,tOH

CS[N,CO]C3d,tOH

Figure 11S. Observed fragmentation reactions upon IR activation of alkali metalized amino acid molecular ions of proline, *N*-methyl proline, *N*-methyl-proline methylester and *N*-methyl alanine (NMA).

$$M^{+}AA \xrightarrow{\text{IRMPD}} \textit{amino acid} + M^{+}$$

AA = amino acid = Proline, *N*-methyl proline,
N-methyl proline methylester,
N-methyl alanine

$M^{+} = Na^{+}, K^{+}, Rb^{+}, Cs^{+}$

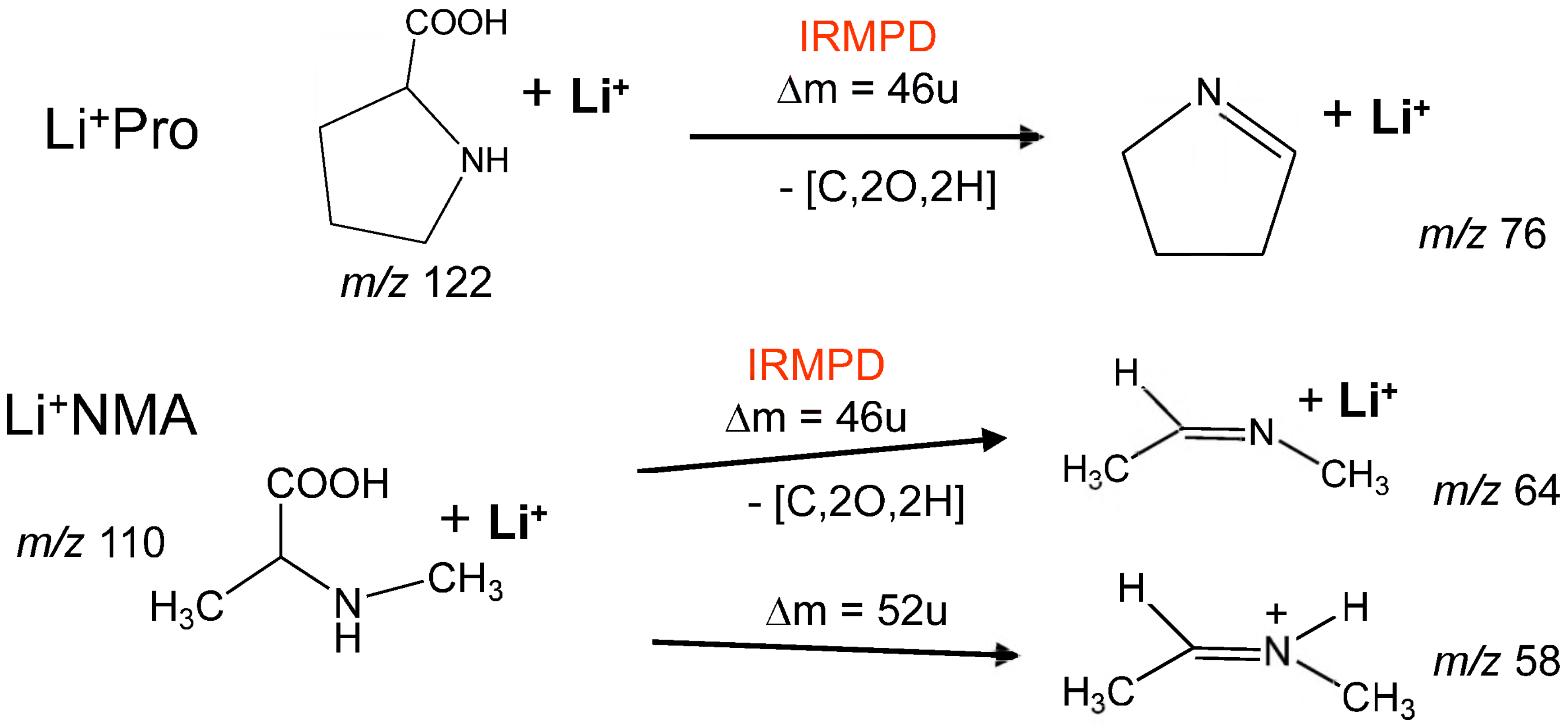

Figure 12S. IRMPD spectrum of K^+*N*-methyl proline methylester and calculated spectra of the two most stable CS isomers computed at the B3LYP/6-311++G(2d,2p) level of theory.

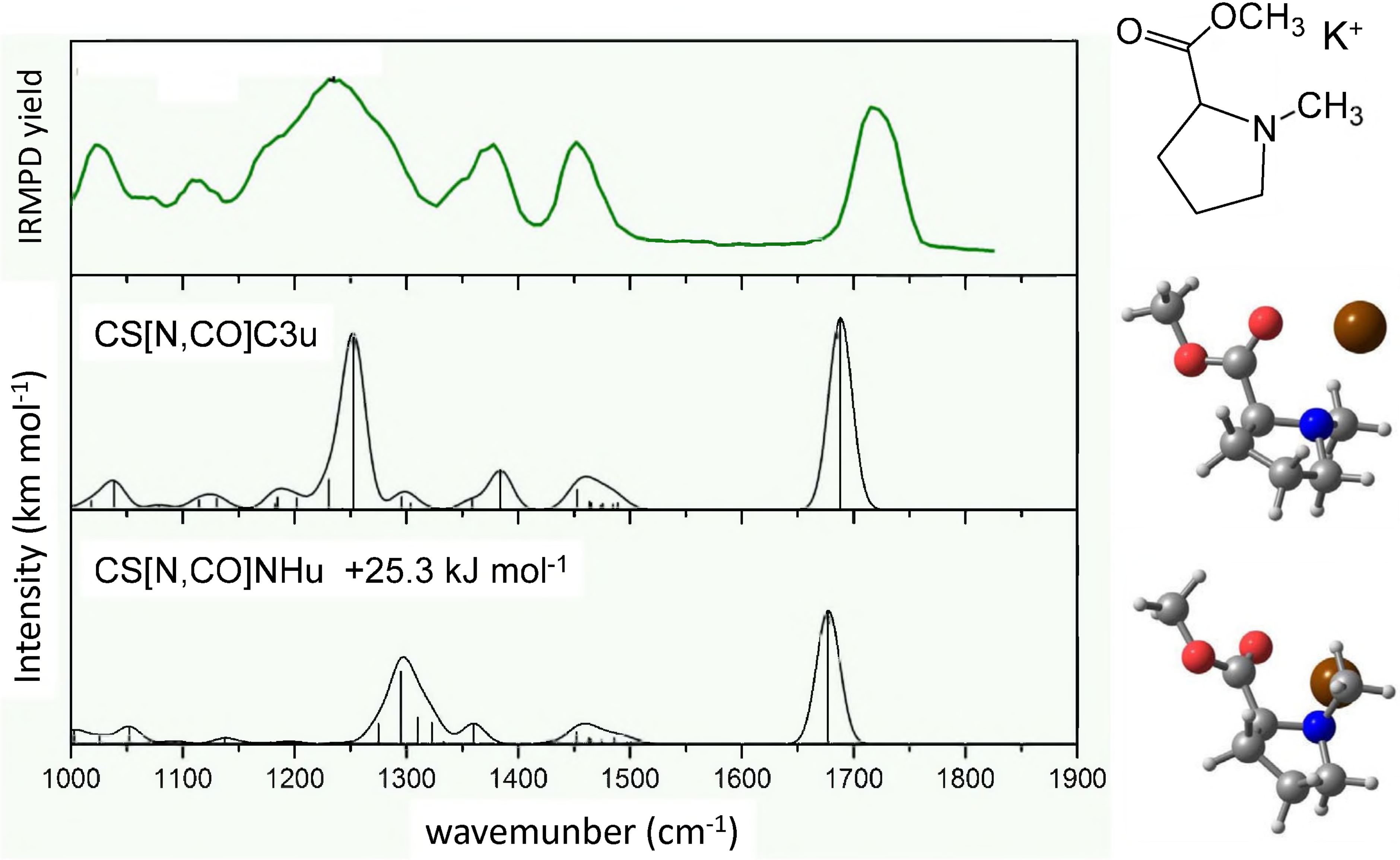

Figure 13S. IRMPD spectrum of Li⁺*N*-methyl alanine and calculated spectra of the two most stable isomers SB[CO_2^-]e and CS[N,CO]e computed at the B3LYP/6-311++G(2d,2p) level of theory.

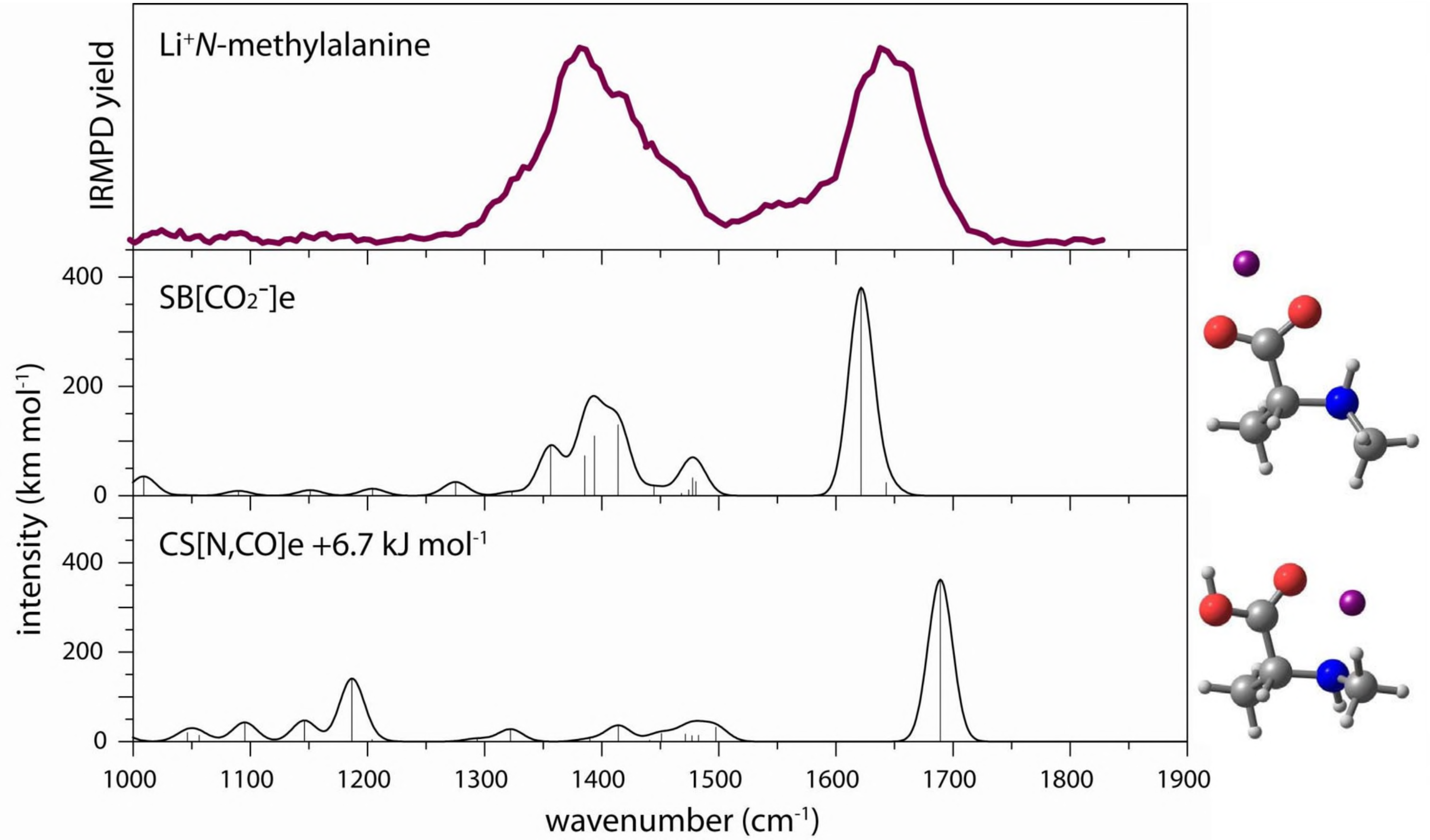

Figure 14S. Lowest energy gas-phase ion structures of Li$^+$*N*-methyl alanine, computed at the B3LYP/6-311++G(2d,2p) level of theory. Relative energies of the respective isomers are listed in Table 2.

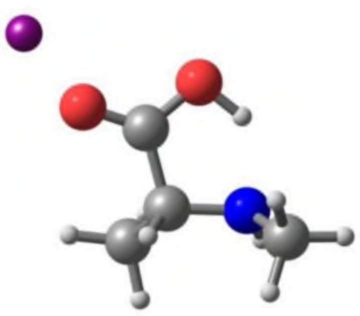

CS[COOH]e

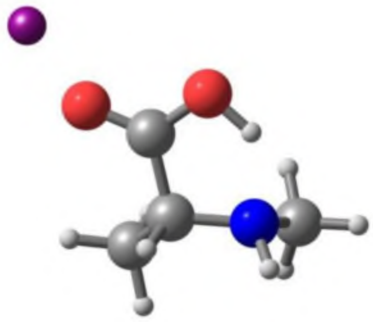

CS[COOH]z

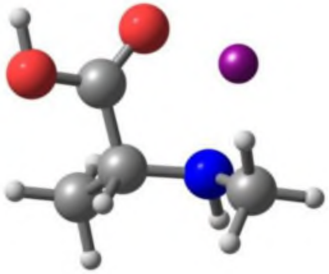

CS[N,CO]e

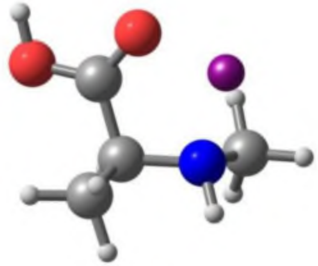

CS[N,CO]z

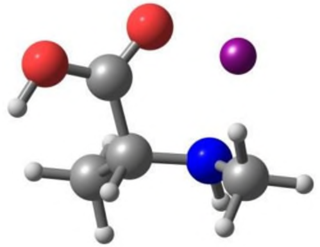

CS[N,CO]OHd,e

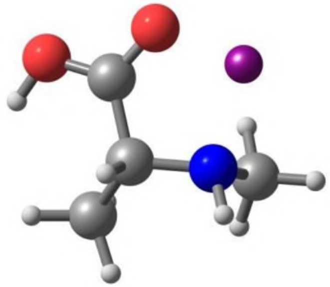

CS[N,CO]OHd,z

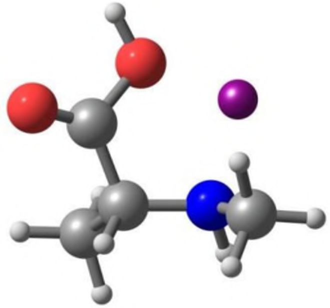

CS[N,OH]e

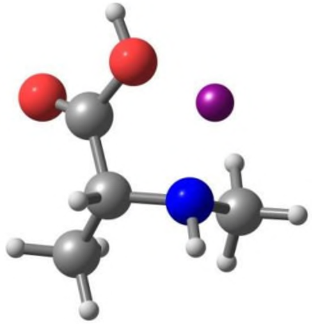

CS[N,OH]z

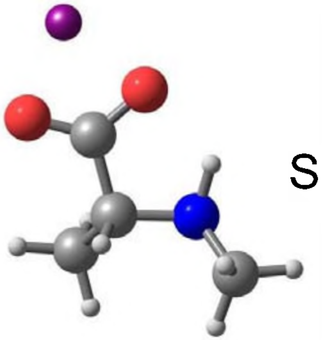

SB[CO$_2^-$]e

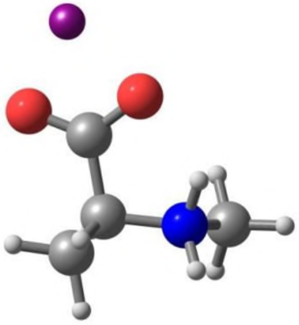

SB[CO$_2^-$]z

Figure 15S. Lowest energy gas-phase ion structures of Na$^+$*N*-methyl alanine, computed at the B3LYP/6-311++G(2d,2p) level of theory. Relative energies of the respective isomers are listed in Table 2.

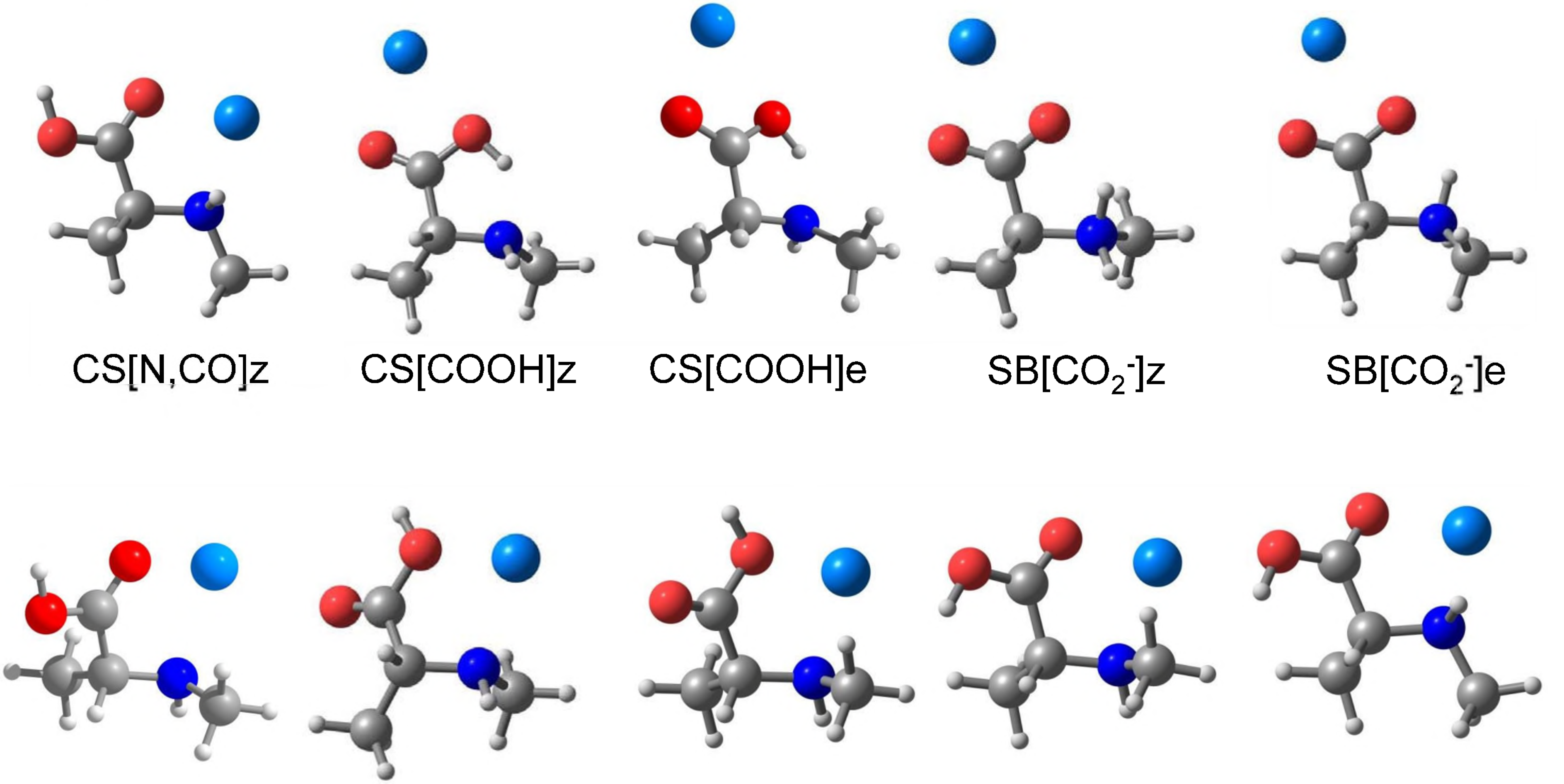

CS[N,CO]z

CS[COOH]z

CS[COOH]e

SB[CO_2^-]z

SB[CO_2^-]e

CS[N,CO]e

CS[N,OH]z

CS[N,OH]e

CS[N,CO]OHd,e

CS[N,CO]OHd,z

Figure 16S. IRMPD spectrum of K^+*N*-methyl alanine and calculated spectra of the two most stable isomers SB[CO_2^-]e and CS[COOH]e computed at the B3LYP/6-311++G(2d,2p) level of theory.

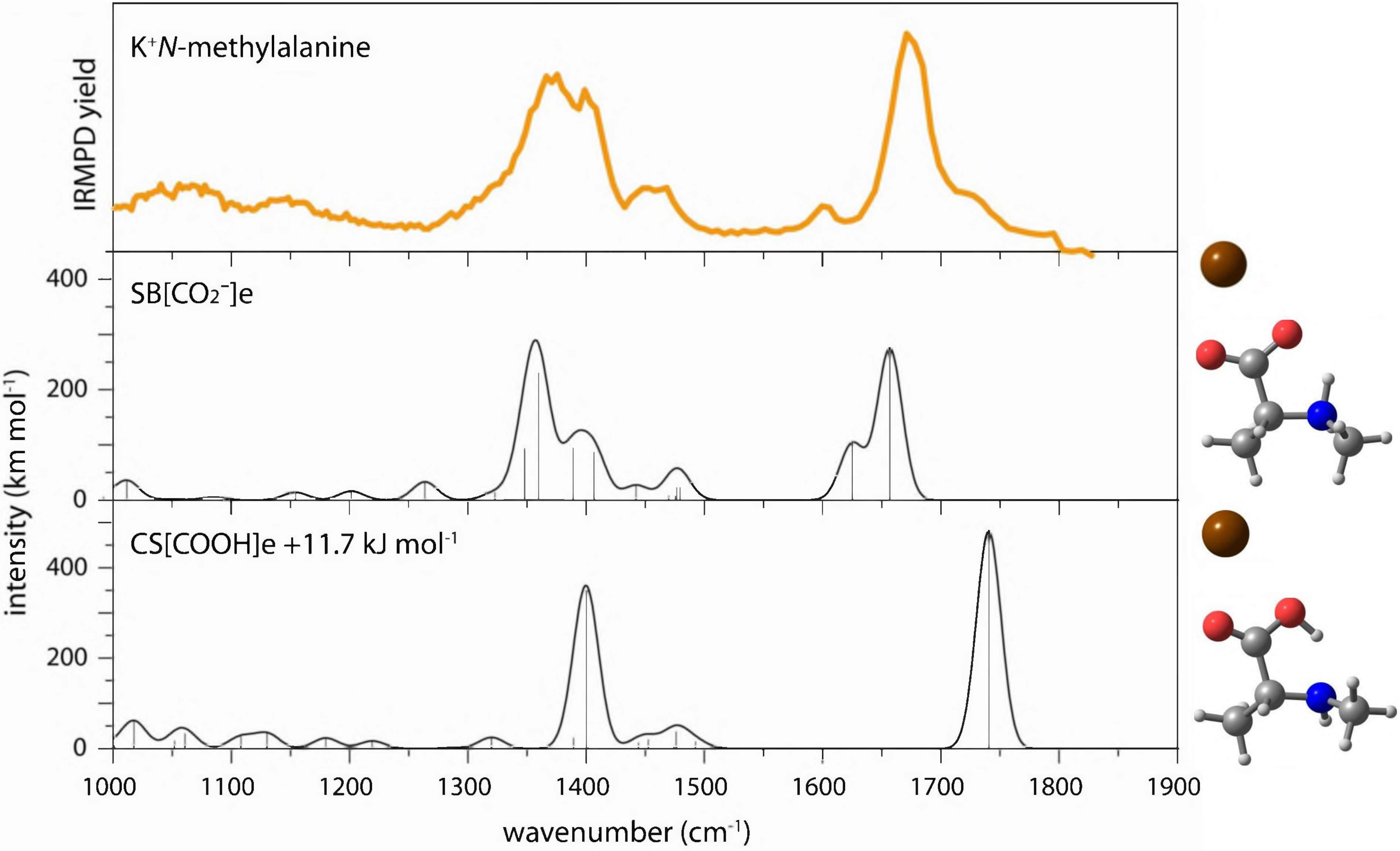

Figure 17S. Lowest energy gas-phase ion structures of K$^+$*N*-methyl alanine, computed at the B3LYP/6-311++G(2d,2p) level of theory. Relative energies of the respective isomers are listed in Table 2.

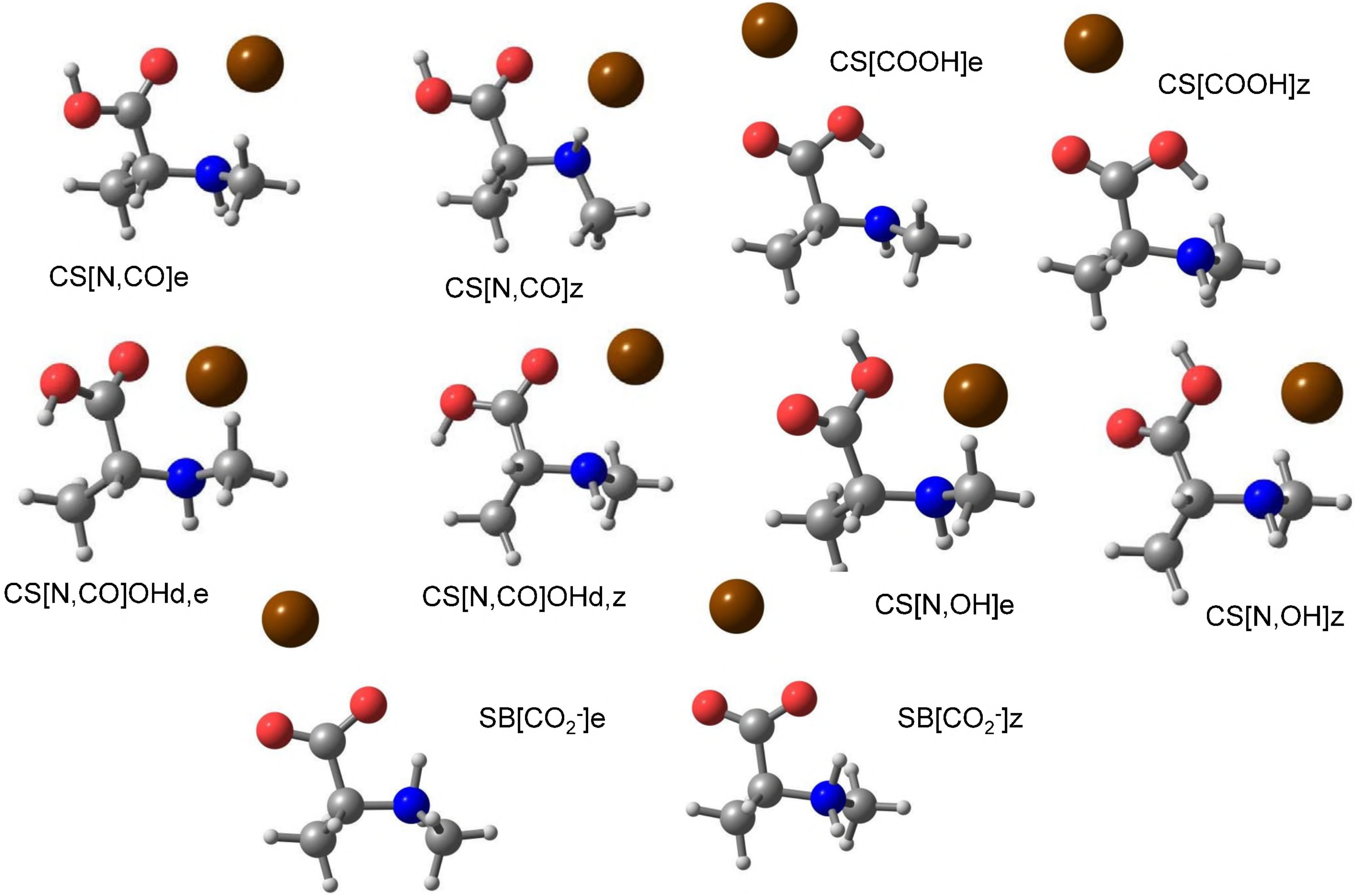

CS[N,CO]e

CS[N,CO]z

CS[COOH]e

CS[COOH]z

CS[N,CO]OHd,e

CS[N,CO]OHd,z

CS[N,OH]e

CS[N,OH]z

SB[CO$_2^-$]e

SB[CO$_2^-$]z

Figure 18S. IRMPD spectrum of Rb$^+$*N*-methyl alanine and calculated spectra of the two most stable SB and CS isomers. All conformers of Rb$^+$*N*-methyl alanine identified by theory are presented in Figure 19S.

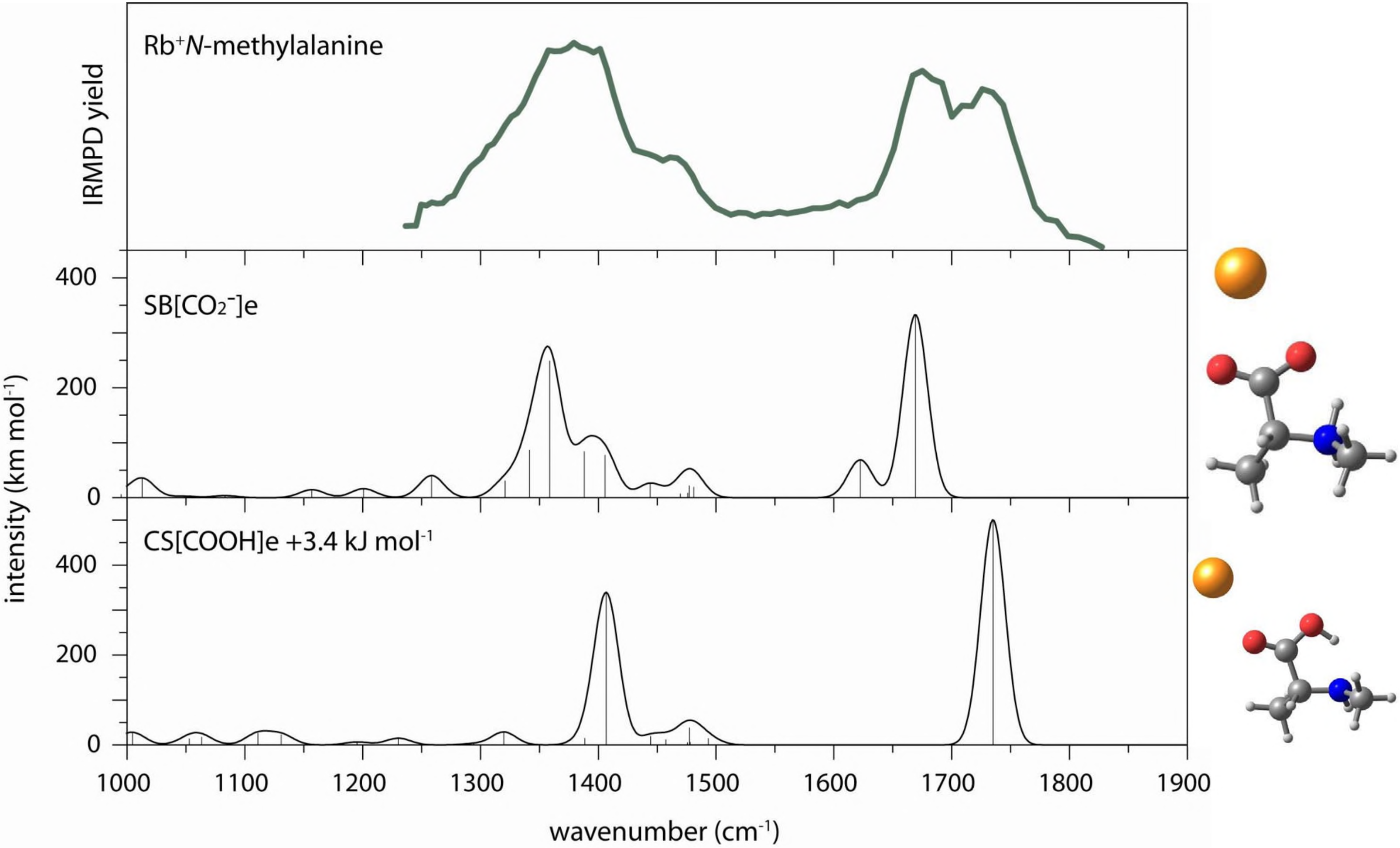

Figure 19S. Lowest energy gas-phase ion structures of Rb^+*N*-methyl alanine, computed at the B3LYP/6-311++G(2d,2p) level of theory. Relative energies of the respective isomers are listed in Table 2.

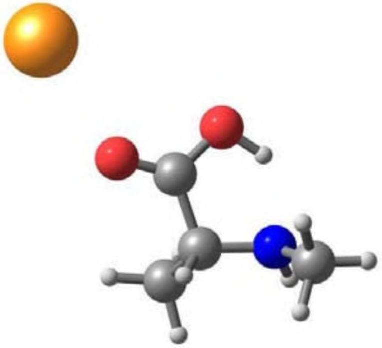

CS[COOH]e

CS[COOH]z

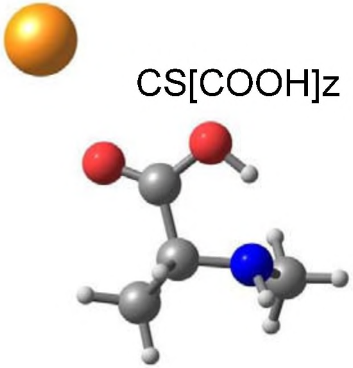

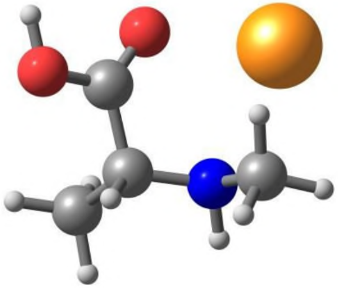

CS[N,CO]e

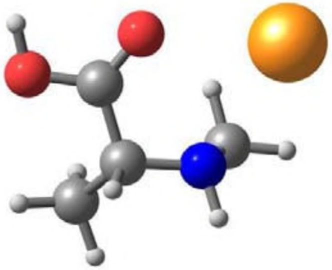

CS[N,CO]z

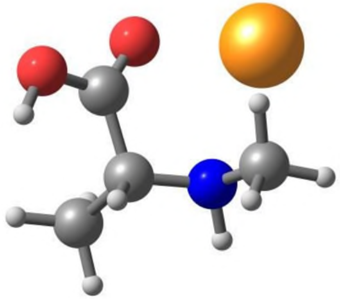

CSCS[N,CO]OHd,e

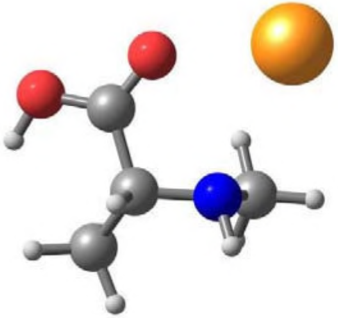

CS[N,CO]OHd,z

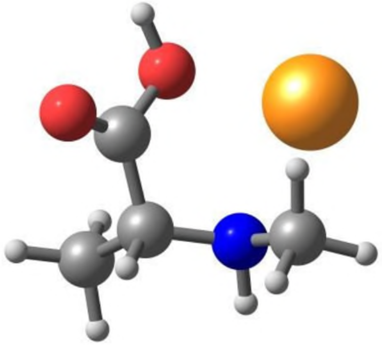

CS[N,OH]e

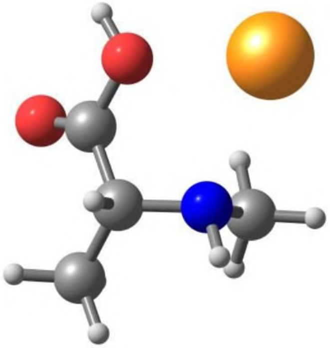

CS[N,OH]z

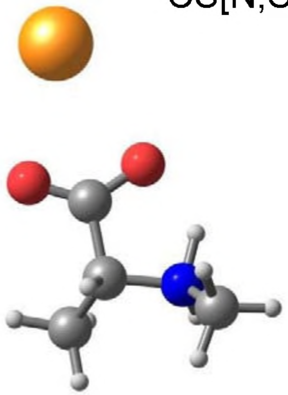

SB[CO_2^-]e

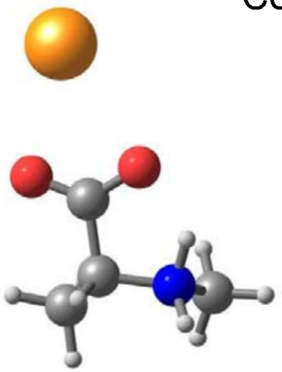

SB[CO_2^-]z

Figure 20S. Lowest energy gas-phase ion structures of Cs^+*N*-methyl alanine, computed at the B3LYP/6-311++G(2d,2p) level of theory. Relative energies of the respective isomers are listed in Table 2.

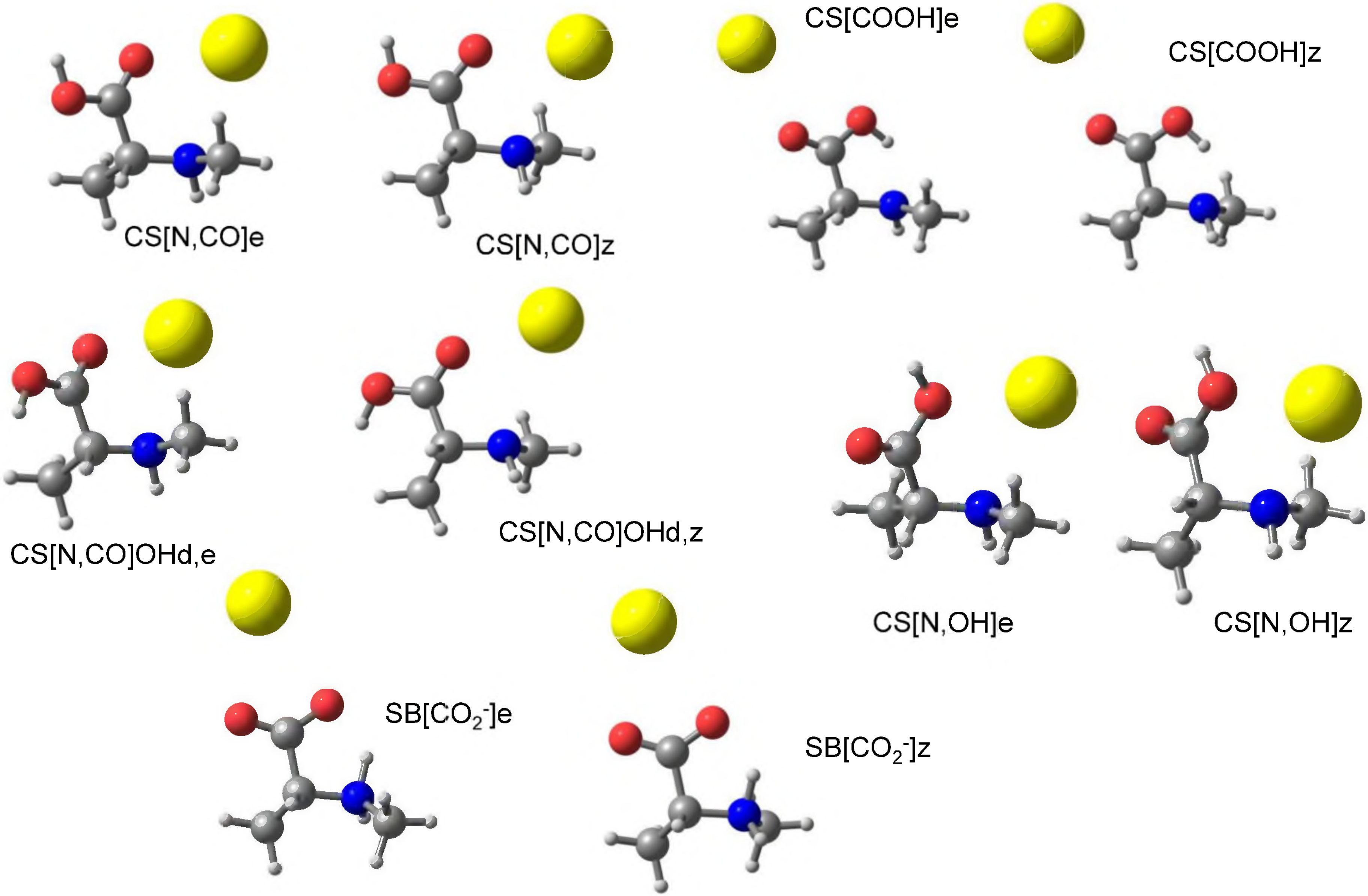

CS[N,CO]e

CS[N,CO]z

CS[COOH]e

CS[COOH]z

CS[N,CO]OHd,e

CS[N,CO]OHd,z

CS[N,OH]e

CS[N,OH]z

SB[CO_2^-]e

SB[CO_2^-]z

Table 1S. Relative energies including ZPE corrections [kJ mol^{-1}] for all conformers of alkali metal ion complexes of *N*-methyl glycine (M$^+$NMG) with M$^+$ = Li$^+$, Na$^+$, K$^+$, Rb$^+$, Cs$^+$ as predicted by B3LYP/6-311++G(2d,2p) calculations.

	Li$^+$NMG	Na$^+$NMG	K$^+$NMG	Rb$^+$NMG	Cs$^+$NMG
SB[CO$_2^-$]	0.00	0.00	0.00	2.17	7.10
CS[COOH]	28.81	19.32	6.75	0.00	0.00
CS[N,CO]	1.43	10.80	11.57	10.32	13.22
CS[N,CO]tOH	24.69	33.42	32.79	30.45	32.10
CS[N,OH]	43.83	50.07	48.17	44.74	46.25
Transition states	27.26	16.12	7.60	4.68	7.23

Table 2S. Relative energies including ZPE corrections [kJ mol^{-1}] for all conformers of alkali metal ion complexes of glycine (M$^+$Gly) with M$^+$ = Li$^+$, Na$^+$, K$^+$, Rb$^+$, Cs$^+$ as predicted by B3LYP/6-311++G(2d,2p) calculations.

	Li$^+$Gly	Na$^+$Gly	K$^+$Gly	Rb$^+$Gly	Cs$^+$Gly
SB[CO$_2^-$]	19.95	8.66	7.98	17.49	22.91
CS[COOH]	→CS[CO]	16.18	1.60	0.90	→CS [CO]
CS[N,CO]	0.00	0.00	1.48	7.75	11.56
CS[CO]	35.00	14.59	0.00	0.00	0.00
CS[N,CO]tOH	22.95	22.92	22.97	28.60	32.00
CS[N,OH]	46.32	42.21	40.00	43.72	46.31
Transition states	59.23	35.74	27.01	31.71	34.66